

Authors' Response to Anonymous Referee #1

We are grateful to the referee for reading our manuscript and we thank for her/his comments.

In the following we reply to each of the referee's comments. We highlight individual parts of the comments that we are going to address in italics. Our response is put below each comment together with our proposed changes to the manuscript; where these changes will appear in the revised manuscript is put in parentheses.

- *page 3, line 19: rho of w (density of water) should be defined here.*
 - Yes, we need to define ρ_w here and will do so in the revision.(page 3, line 19)
- *p.3, l.26 “For faster computation...” - faster than what? Please clarify.*
 - We meant faster computation because of the daily time step. Of course this is relative, so we will delete that phrase and instead simply state: *We use a time step of one day.* (p.3, l.26)
- *p.5, l.15: please add comma after “A set to zero”.*
 - We will add a comma to clarify that sentence. (p.5, l.15)
- *p.6, l.3 water density is defined here but should be defined earlier on p.3 (see above).*
 - In the revised manuscript, ρ_w should be already defined before as mentioned in the first bullet point.
- *p.6, l.18 “We neglect refreezing of melted ice and treat ice melt as runoff.” - what is the basis of this assumption? Is it reasonable and realistic for the GrIS? Adding a sentence or two of justification here would be helpful.*
 - Ice itself does not retain any meltwater at the surface and we assume that it has a water holding capacity of effectively zero. If a snow pack is present we assume that it can retain melt water. However, it turns out that we have missed adding a refreezing fraction f_R to the rhs of Eq. (16c), which reduces the potential refreezing according to this parameter. In the revised manuscript f_R is one of the free model parameter and included in the parameter calibration (varying between 0 and 1).
 - In the revised manuscript Eq. (16c) should read: $R = R_{\text{rain}} + R_{\text{melt}} = f_R(R_{\text{pot, rain}} + R_{\text{pot, melt}})$ with f_R being the refreezing fraction and a free model parameter.
 - To explain the neglect of refreezing of melted ice, we suggest the two sentence from above: Ice itself does not retain any meltwater at the surface and we assume that it has a water holding capacity of effectively zero. If a snow pack is present we assume that it can retain melt water. (to be added to p.6, l.18)
- *p.7, l.8: “Tmin is set to 263.15K as originally proposed” - How reasonable is this assumption and is it supported by in situ and/or satellite data? What is the sensitivity of model results to varying it by several degC plus and minus?*
 - After revising the albedo parameterisation we decide not to use the proposed approach by Slater et al. (1998). We find that $\alpha_{s,\text{max}}$ and $\alpha_{s,\text{min}}$ are only a couple of per cent apart of each other, (0.77 and 0.80, respectively in the submitted manuscript, see Table 1). This means that the overall effect of this parameterisation will be at max 3 per cent, which is not much added value in our opinion. Instead, we decided to reduce the complexity of the albedo parameterisation and the number of free model parameters. Hence, $\alpha_{s,\text{min}}$ and T_{min} are no longer needed. However, for other (future) application we keep the albedo in the model to be chosen by the user optionally but will not mention it in the manuscript to avoid confusion.
 - We propose to simplify Sect 2.4 (Snow albedo parametrisation) in the manuscript. The albedo parameterisation simplifies to $\alpha = \alpha_s - f_a(\alpha_s - \alpha_{bg})$, i.e., Eq. (19). Eq. (18a,b) are no longer needed. Changes in Sect. 2.4 and throughout the revised manuscript will be made accordingly. (Sect. 2.4, p7-8)
- *p.8, l.1 reword to “we refrain FROM USING...”*
 - We will revise this part of the manuscript because of justified comments by the second referee, who suggests to use more than three years for the calibration to make a more robust parameter estimation. (p.8 ll.1-4)
- *p.8, l.15 -> “are close TO their expected trajectories.”*
 - We will change the sentence as proposed.
- *p.8, l.24: -> “while also allowing THE ASSESSMENT OF variables with different units.”*

- We will change the sentence as proposed.
- *p.10, ll.4/5: “While melting over the northern part of the ice sheet is overestimated by SEMIC, it is underestimated over the southern part of the ice sheet” - this seems opposite to what I interpret from studying Figure 3 - please check.*
 - No, the difference between SEMIC and MAR is positive in the northern part and negative in the southern part of the ice sheet. Here, melt is defined as positive quantity, although the loss of mass by melt is negative in a physical sentence. But apparently this is confusing so we suggest to add a sentence here. For example this might be helpful:
 - Note that melt is defined as a positive quantity but is subtracted from the surface mass balance (p.10 ll.5)
- *p.11, l.8: -> “However, the surface mass balance itself is less sensitive to A than melting.”*
 - We will change the sentence as proposed.
- *p.19, Figure 3 caption -> “The outlined contours SHOW the boundaries...”*
 - We will change the sentence as proposed.

Mario Krapp (on behalf of the authors)

Authors' Response to Xavier Fettweis

We thank Xavier Fettweis for his helpful comments and for the pointing out the clear distinction between MAR and its snowpack model. Xavier raised some valid points which we would like to address in our revised manuscript.

In the following we reply to each of the referee's comments. We highlighted individual parts of the comments that we are going to address in italics. Changes in the manuscript have been described and highlighted in italics; where these changes appear in the updated manuscript is put in parentheses.

1. Reference to MAR in the text

- [...] *SEMIC is comparable in fact to the snow model used in MAR [...] and [...] all the inter-comparisons of Surf Temp. and SMB components with MAR must refer to SISVAT (used in the MAR model) and not to MAR!*
 - We acknowledge that MAR is more than just the surface energy and mass balance model but we think that we already differentiate between SEMIC and MAR right in the beginning. For example, in the abstract we write that SEMIC is able *to reproduce surface characteristics and day-to-day variations similar to the regional climate model MAR* and that SEMIC is *in good agreement with the more sophisticated multi-layer snowpack model included in MAR*. For the sake of clarity and understanding we simply use the model name MAR whenever we refer to the surface snowpack model (i.e., SISVAT). However, to give reasonable credit to the MAR community should add a brief description what we exactly compare our model to.
 - We propose to add a brief description of SISVAT and its part in the MAR framework in Sect 2.5 (page 7). However, throughout the paper we are still simply referring to MAR output whenever a comparison to SEMIC is made.
- *Secondly, SEMIC does not allow to take into account the atmosphere-snowpack interactions. But, as it is forced by MAR, these feedbacks (and notably the albedo feedback) are taken into account here. This should be mentioned in the manuscript.*
 - That is true in the sense that atmospheric characteristics are prescribed and are not affected by surface properties simulated by SEMIC. This is because in this work we used MAR output for testing of SEMIC. However, since SEMIC calculates surface-atmosphere heat fluxes such latent heat, sensible heat, and upward longwave radiation, in the future it is planned to couple SEMIC bi-directionally with an appropriate atmosphere model. Then atmosphere-snowpack interaction will be properly accounted for.
 - However, we will add a brief explanation that the current setup only serves the purpose of mimicking the response of SEMIC to an atmosphere forcings but that the surface response cannot be not taken into account by the atmosphere.
- *Thirdly, it is true that MAR is very slow in respect to SEMIC [...] due to the physical atmospheric downscaling. [...] This should be mentioned in the manuscript.*
 - We do not want to blame MAR in terms of runtime. But explaining why a regional climate model needs more computational time is not within the scope of our paper. However, we can make clear that SEMIC and MAR are two different classes of models and we will add sentence about the distinction in the part above (Sect. 2.5).
- *Finally, the SISVAT snow model as well as the raw CROCUS snow model can be run in stand alone mode like SEMIC. Therefore, this shows well that this paper is well SEMIC vs CROCUS and not SEMIC vs MAR.*
 - We use the term MAR for simplicity but will stick to it, also because SISVAT is a component of the MAR model (see our first bullet point).

2. Calibration with MAR outputs only

- *I am a bit surprised that the calibration was only made over three years [...]. But 3 yrs is very short and a validation [...] over both 10 yrs periods (2090-2100 and 1990-2000) will be more robust.*
 - We agree that a longer calibration period over both, present-day and future-warming conditions is more robust and would lead to more robust optimal parameter estimate. We changed the forcing data for the proposed periods, 1990-2000 and 2090-2100, but because of the computational overhead we used just a subset of the MAR data, i.e., a random sub-sample accounting for 20% of land and ice points.
 - The calibration procedure will be thoroughly revised and extended in Sect. 3, Model parameter calibration (page 8).
- *[...] the sensitivity of the bare ice albedo value is not tested. In MAR, this one is the more sensible parameters (as explained in Fettweis et al., 2016). As SEMIC underestimates melt in respect to MAR, lower values of bare ice albedo can reduce this bias.*
 - Yes, the bare ice albedo has not been tested. We will add the sensitivity of bare ice albedo α_i , as well as of bare land albedo α_l , and the missed f_R to Sect. 3.4, Parameter Sensitivity (p. 10-11). Figure 6 will be also updated accordingly (page 22).
 - Note, that we will no longer use the Slater et al. (1998) albedo parameterisation (for reasons, see our response to referee #1). Therefore, $\alpha_{s,\min}$ will no longer be part of the sensitivity in Figure 6 (page 22) and the text (p. 10-11).
- *MARv2 [...] overestimates the melt in respect to MARv3.5.2. A calibration/validation over current climate using the SMB PROMICE data set will be more robust. [...] I don't ask to recalibrate SEMIC over current climate using the SMB PROMICE data set but this issue should be at least mentioned in the manuscript.*
 - We know that with each model update several aspects of that model are being improved. However, with this paper we show that SEMIC can be a surrogate of a sophisticated snow-pack model and we prove it. The parameters will likely change if forced with different data and calibrated for different data.
 - We will add a brief discussion of this issue in Sect. 5, Discussion (p. 13-14).

3. Cumulated SMB change

- *SEMIC seems to diverge from MAR after 2050. What are the total cumulated differences in 2100? For me, the calibration should be made to have the same cumulated SMB changes over 2000-2100 than MAR and not to have good results over 2098-2100 only. Due to error compensations, having a too high/too low SMB several years in respect to MAR is not a problem for an ice sheet model which will give the same results at the end than if it will be forced by MAR. The best will be to calibrate SEMIC over current climate when we have other estimations of cumulated SMB changes than MAR (van den broeke et al., TC, 2016).*
 - Yes, SEMIC diverges from MAR in the RCP8.5 scenario. We aim to be as close to MAR results as possible. But we cannot use the whole period of MAR data (i.e., 1970-2100) to calibrate our model. First, we need to strictly differentiate between training data and test data. We do so by defining the periods 1990-2000 and 2090-2100 as our training data. Second, it is computationally not feasible to use all MAR model years for the parameter calibration, which needs to be run several tens of thousands of times.
 - There is a valid point in this comment. That is to quantify the differences between SEMIC and MAR over time, i.e., the cumulative difference. For that reason we can add a figure, similar to Fig. 4, but showing the cumulative differences of mass balance terms over time, e.g., for the whole period 1970-2100 or for the historical and RCP8.5 period separately.

Minor Remarks

- *Fig 2: the SMB zones shown in Fig 2 were only valid over the 1990's [...] J. These boundaries are already no more relevant for current climate of the 2000's. This issue should be mentioned in the manuscript.*
 - We use the zones only to differentiate the major climatic regimes across the Greenland Ice Sheet. For example, on page 9, ll.3 we point out that the *regions crudely represent the main ablation zones at the ice-sheet margins (region 1), the main accumulation zone at ice-sheet interior*. However, we will remark here that the regions only represent different SMB zones for today's climate and may not be valid for any future warming scenario such as RCP8.5. (Sect 3.1, p. 9)
 - The only distinction SEMIC makes is between ice-covered and ice-free zones, i.e., land/ice mask. We will also add a remark to Fig. 2 to explain that the differentiation is only valid for present day. (page 18)
- *Fig 3: MAR/ERA-40 must be SISVAT/CanESM2. It should be interesting to show the differences over current climate (in supplementary material) when MAR is forced by reanalysis. This error in the legends means that such a comparison has already been done.*
 - Indeed, MAR/ERA-40 output has been used at an earlier stage of our research. However, to minimize the number of different datasets used for that study, we decided to solely focus on MAR/CanESM2 output for our calibration and validation process. The error in the legend has been changed accordingly.
- *Fig. 5: not useful => supplementary material.*
 - We disagree, while the maps in Fig. 3 provides a visual for the spatial (but time-averaged) differences between MAR and SEMIC, Fig. 5 provides a visual for the temporal differences between the two models. Having both figures in the main text will provide a more complete picture of SEMIC and MAR, both in space and time.
- *Fig. 8: showing an equivalent of Fig 4 with cumulated values will be more useful.*
 - This will be shown in a new figure that depicts the cumulative differences between SEMIC and MAR (see our last bullet point in the comment section 3, cumulated SMB changes).

Mario Krapp (on behalf of the authors)

Response to the Editor

- 1) *I would like to ask you to consider, if possible, to add something to the title that suggests that the model here proposed is calibrated using MAR outputs. This should also be stressed (with this aspect more important than the title) in the text, especially in the discussion and conclusions sections. The outputs of the regional climate model used to calibrate the model are heavily dependent on the version used (here 3.2) and the forcing. The authors need to highlight this and, particularly, that the model can reproduce MAR outputs but care should be taken to claim the validity of SEMIC as presented in this study. Also, it would be important for the authors to suggest how the model can be used in a more general way and what would be the impact of using different MAR (or RACMO ?) versions on the results.*
 - We agree that the contribution of Xavier Fettweis and the MAR team should be acknowledged thoroughly. We explain in the beginning of the discussion how valuable the publicly available MARv2 data are and, as you suggested, that MARv2 is somehow outdated and any results from SEMIC should be taken with a grain of salt
 - We also add to the conclusion that SEMIC has been forced with atmospheric fields from MARv2 and our comparison is mainly done with its surface model SISVAT (also suggested by Xavier in his review)
- *The other point is that the authors offer no validation of the results using in-situ measurements. Is this something that can be at least discussed ?*
 - Actually, we did a preliminary analysis (before submitting the paper) for which SEMIC has been forced by meteorological data (Morin et al., 2012) but we didn't want to include this analysis in the first place because i) we think it would make the paper even more complicated and bloated, and ii) that the reader might miss the point of describing SEMIC in detail. We think a comprehensive comparison using SEMIC with different types of climate datasets, e.g., other regional climate models (or MAR versions), re-analysis data, or other in-situ observations (e.g., PROMICE or GC-NET) would be a nice follow-up study.
 - We now mention in the discussion that we did a preliminary analysis (with the Morin et al. (2012) dataset) but provide no further details.
- 2) *the second important point is that the paper lacks of appropriate references. I would strongly encourage the authors to update them and increase their number. This should be done throughout the paper. As an example (though, again, the authors should check through the whole paper), in Section 3 there is no justification or reference for choosing the snow height to 1 m. Also, references to previous work concerning snow energy balance should be added together with those referencing to the origin of equations used and the choices made (as, for example, the case mentioned above). again, this should be properly done throughout the paper.*
 - We agree and add appropriate references where needed, namely in the discussion, the model setup section, and in the discussion
 - Additional references:
 - * Franco et al.: Future projections of the Greenland ice sheet energy balance driving the surface melt, *The Cryosphere*, 7, 1–18, 2013.
 - * Fettweis et al.: Reconstructions of the 1900–2015 Greenland ice sheet surface mass balance using the regional climate MAR model, *The Cryosphere Discussions*, 2016, 1–32, 2016.
 - * van As et al.: Placing Greenland ice sheet ablation measurements in a multi-decadal context, *Geological Survey of Denmark and Greenland Bulletin*, 35, 71–74, 2016.
 - * Noel et al.: Evaluation of the updated regional climate model RACMO2.3: summer snowfall impact on the Greenland Ice Sheet, *The Cryosphere*, 9, 1831–1844, 2015.
 - * Dee et al.; The ERA-Interim reanalysis: configuration and performance of the data assimilation system, *Quarterly Journal of the Royal Meteorological Society*, 137, 553–597, 2011.
 - * Morin et al.: An 18-yr long (1993–2011) snow and meteorological dataset from a mid-altitude mountain site (Col de Porte, France, 1325 m alt.) for driving and evaluating snowpack models, *Earth System Science Data*, 4, 13–21, 2012.
 - * Oerlemans, J.: The mass balance of the Greenland ice sheet: sensitivity to climate change as

revealed by energy-balance modelling, *The Holocene*, 1, 40–48, 1991.

- * Oerlemans, J. and Knap, W.: A 1 year record of global radiation and albedo in the ablation zone of Morteratschgletscher, Switzerland, *Journal of Glaciology*, 44, 231–238, 1998
- * Bougamont et al.: Impact of model physics on estimating the surface mass balance of the Greenland ice sheet, *Geophysical Research Letters*, 34, L17 501, 2007.
- * Greuell et al.: Modelling land-ice surface mass balance, p. 117–168, Cambridge University Press, 2004.
- 3) *Figures dont have labeling for each panel. These should be added and captions should be changed accordingly. figures 5 and 6 are not clearly legible. It is impossible to separate between the MAR- and SEMIC-modeled quantities. Authors should improve these figures. Figure 7 is missing units on the left panels. Also, units are usually reported in square parentheses. Figure 10: ‘lighter colours’ is not a good reference for readers. Authors should include a label or similar to indicate the different quantities associated with the colors.*
 - We add labels to Figures 1, 3, 4, 7, 8, 9, and 10.
 - We hope that Figures 5 and 6 are better legible as we increased font size and use slightly transparent and thinner lines.
 - Units now appear in squared brackets.
 - Figure 10 has distinguishes SEMIC and MAR using different line styles, with appropriate labels added.

Mario Krapp (on behalf of the authors)

List of all relevant changes

Changes as requested by the reviewers:

- We mention the snowpack model SISVAT in the abstract and in the Model Setup (Sect. 2.5)
- We add a sentence to specify that air density is not computed by MAR but derived from the ideal gas law
- We add the model parameter f_R into the model equations (Sect. 2.3) and throughout the manuscript
- The snow albedo parameterisation has been simplified (Sect 2.4)
- The model setup was rewritten to account for the different (historical and RCP8.5) and longer calibration period (Sect 2.5) and a slightly different calibration setup
- Accordingly, the new calibration periods have been added to the Model calibration (Sect 3)
- An error in the centred root mean square definition has been corrected (Eq. 19)
- The model calibration setup led to a new optimal parameter set, which has been updated in Sect 3.1 and Table 3
- Characteristic ice-sheet variables and differences to MAR have changed because of the new optimal parameter set and numbers have been updated in Sect 3.3 and Table 4
- The parameter sensitivity has been simplified and only accounts for the overall cost function J ; Sect 3.4 has been rewritten therefore
- The discussion has been updated to reflect the major changes in model setup and its calibration
- Maps and plots which showed the single previous calibration period do now show both periods, 1990-1999 and 2090-2999: Figs 3 & 4, Figs. 5 & 6, Fig. 7, Fig. 9

Changes as requested by the editor:

- We explain in the discussion that MARv2 is outdated and any results from SEMIC should be taken with a grain of salt
- We add to the conclusion that SEMIC has been forced with MARv2 atmospheric fields and that the comparison has been done with MAR's surface module SISVAT
- We add a sentence about SEMIC and its potential application to different types of climatic data, e.g., re-analysis or in-situ observations and that we did some preliminary analysis with meteorological forcing data from Col de Porte (Morin et al., 2012)
- We add 10 additional reference in the introduction, the model setup, and the discussion to increase the actual number of references and to support some claims we made throughout the respective parts of the manuscript
- We add appropriate labels to the figures
- Units are displayed in square brackets
- We improved figure 5 and 6 to increase their readability
- We changed the line style for MAR in Fig. 10 and add an appropriate label to the figure

SEMIC: An efficient surface energy and mass balance model applied to the Greenland ice sheet

Mario Krapp^{1,2}, Alexander Robinson^{3,1}, and Andrey Ganopolski¹

¹Potsdam Institute for Climate Impact Research

²Department of Zoology, University of Cambridge

³Dpto. Astrofísica y CC de la Atmósfera, Universidad Complutense de Madrid

Correspondence to: mariokrapp@gmail.com

Abstract. We present SEMIC, a Surface Energy and Mass balance model of Intermediate Complexity for snow and ice covered surfaces such as the Greenland ice sheet. SEMIC is fast enough for glacial cycle applications, making it a suitable replacement for simpler methods such as the positive degree day method often used in ice sheet modelling. Our model explicitly calculates the main processes involved in the surface energy and mass balance, while maintaining a simple interface and minimal data input to drive it. In this novel approach, we parameterise diurnal temperature variations in order to more realistically capture the daily thaw-freeze cycles that characterise the ice sheet mass balance. We show how to derive optimal model parameters for SEMIC to reproduce surface characteristics and day-to-day variations similar to the regional climate model MAR (Modèle Atmosphérique Régional, [version 2](#)) and its incorporated multi-layer snowpack model [SISVAT \(Soil Ice Snow Vegetation Atmosphere Transfer\)](#). A validation test shows that SEMIC simulates future changes in surface temperature and surface mass balance in good agreement with the more sophisticated multi-layer snowpack model [SISVAT](#) included in MAR. With this paper, we present a physically-based surface model to the ice sheet-modelling community that is computationally fast enough for long-term integrations, such as glacial cycles or future climate change scenarios.

1 **Introduction**

1 Introduction

Currently, surface melt accounts on average for about half of the observed Greenland ice sheet loss; the other half is lost through basal melt and ice discharge across the grounding line, i.e., calving (van den Broeke et al., 2009). Recent observations show that Greenland's surface mass balance is further declining (Hanna et al., 2013). The positive surface mass balance can no longer compensate losses via ice discharge and is therefore regarded as a dominant source of Greenland's total mass loss. The extreme melt season in 2012 exposed the Greenland ice sheet's vulnerability to long-lasting temperatures anomalies (Nghiem et al., 2012). As more marine terminating glaciers further retreat (Thomas et al., 2011), the partitioning of ice loss is likely to shift further towards the declining surface mass balance.

Numerical simulations of large land ice masses, such as the Greenland and the Antarctic ice sheets, require numerical models to be fast because the response time of ice sheets to changes in the surface mass balance is slow, on the order of years to tens of

millennia (Cuffey and Paterson, 2010). Hence, many thousands of years of model integration are required to spin-up the model or to simulate one or several glacial cycles.

The simplest, fastest, and still most widely used method to estimate the surface mass balance of glaciers and ice sheets is the so-called positive-degree-day (PDD) approach (e.g. Reeh, 1991; Ohmura, 2001). It is based on the empirical relationship 5 between surface melt rate and daily mean surface air temperature. Although PDD parameters are tuned to correctly represent present-day melting rates, past climates may require different parameter values. For instance, the PDD approach with its present-day parameter values is not applicable to orbitally-forced climate change (van de Berg et al., 2011; Robinson and Goelzer, 2014).

The importance of climatic changes in the past to the sensitivity of the Greenland ice sheet has already been acknowledged in 10 one of the first attempts to utilise an energy-balance model for a sensitivity study (Oerlemans, 1991). Under a warming climate an energy-balance approach is superior to the relatively simple PDD method and "snowpack properties evolve on a multidecadal timescale to changing climate, with a potentially large impact on the mass balance of the ice sheet" (Bougamont et al., 2007).

Here, we propose a physically-based model utilising an energy balance approach that is inherently consistent with a variety of climate states different from today, e.g., future warming, last glacial maximum, or the Eemian interglacial. Our proposed 15 model not only accounts for temperature changes but also for changes in other climate factors, such as insolation, turbulent heat fluxes, and surface albedo.

The Surface Energy and Mass balance model of Intermediate Complexity (SEMIC) is based on a surface scheme that has already been used to study glacial cycles (Calov et al., 2005). SEMIC provides a process-based relationship between surface 20 energy and surface mass balance changes. The approach described here guarantees a consistent treatment of melting and meltwater refreezing; both are important processes for the mass budget of ice sheets (Reijmer et al., 2012).

Compared to more sophisticated multi-layer snowpack models, which include snow metamorphism or vertical temperature profile calculations (e.g., Vionnet et al., 2012), SEMIC has a reduced complexity, one-layer snowpack. This saves computation time and allows for integrations on multi-millennial time scales. SEMIC calculates the daily surface energy and mass balance throughout the year but is also fast enough to focus on longer time scales when climatological changes determine the trend of 25 the surface energy and mass balance.

Numerical ice sheet models need the annual mean surface temperatures and annual mean surface mass balance of ice as boundary conditions at the surface. Both are calculated by SEMIC, which can thus be directly coupled to the ice sheet model. There is a multitude of possible applications for SEMIC, for example, under projections of future warming for the next centuries 30 or glacial cycle simulations. In this paper, we will discuss the future warming projections of the RCP8.5 scenario (Moss et al., 2010) to demonstrate the capabilities of our model.

The paper is organised as follows. In the next section, we present the model equations and their parameters. In Sect. 3, we describe the calibration procedure used to constrain the free model parameters and we estimate the sensitivity of the calculated surface mass balance with respect to the model parameters. In Sect. 4, we validate our model against regional climate model data for a future warming scenario. We discuss our findings in Sect. 5 and conclude in Sect. 6.

With this paper we acknowledge, support, and encourage research that follows standards with respect to scientific reproducibility, transparency, and data availability. The model source code and the authors' manuscript source is freely available and accessible online.

2 Model Description

5 SEMIC is based on the calculation of the mass and energy balance of the snow and/or ice surface (see, for example Greuell et al., 2004).

We assume that the surface temperature T_s responds to changes in the surface energy balance according to

$$c_{\text{eff}} \frac{dT_s}{dt} = (1 - \alpha) SW^{\downarrow} + LW^{\downarrow} - LW^{\uparrow} - H_S - H_L - Q_{\text{M/R}} \quad (1)$$

where α is the surface albedo, SW^{\downarrow} is the downwelling shortwave radiation, $(1 - \alpha) SW^{\downarrow}$ is the net shortwave radiation

SW_{net} , LW^{\downarrow} is the downwelling longwave radiation, LW^{\uparrow} is the upwelling longwave radiation, H_S and H_L are the sensible

10 and latent heat flux to the atmosphere, and $Q_{\text{M/R}}$ is the residual heat flux available the energy flux related to phase transitions,

i.e., for melting or refreezing of snow and ice. The parameter c_{eff} denotes the effective heat capacity of the snowpack. In a strict

sense of the term “energy balance” the left-hand-side of Eq. (1) should be zero. Here, we assume that surface temperature and the energy are not in equilibrium because the snowpack or surface exerts some thermal inertia.

Temperatures of snow- and ice-covered surfaces cannot exceed 0° C. However, for computational purposes, we initially

15 assume that T_s represents the potential temperature, which would be observed in the absence of phase transitions, i.e., melting

or refreezing. Once, melting and refreezing has been computed (see Sect. 2.3), the residual heat flux $Q_{\text{M/R}}$ in Eq. (1) keeps track of any heat flux surplus or deficit and is added back to the energy balance. This way, T_s never exceeds 0° C over snow

and ice.

For coupling to an ice sheet model, the surface mass balance for ice (SMB_i) is computed by SEMIC. It separates the total

20 surface mass balance into the surface mass balance for snow and for ice:

$$SMB = SMB_s + SMB_i = P_s - SU - M + R, \quad (2)$$

$$SMB_s = P_s - SU - M_{\text{snow}} - C_{si}, \quad (3)$$

$$SMB_i = C_{si} - M_{\text{ice}} + R. \quad (4)$$

Here, P_s is the snowfall rate and SU is the sublimation rate which is related to the latent heat flux via $H_L / \rho_w L_s$, with ρ_w and

25 L_s being water density and latent heat of sublimation, respectively (see Table 1). The model variable M is the total melting

rate, i.e., the sum of snow and ice melt (denoted by the subscripts), R is the refreezing rate of liquid water (rain or melt water),

and C_{si} is the compaction rate of snow which is turned into ice.

Changes in snowpack height h_s (in meter water equivalent) are determined by the surface mass balance of snow:

$$\frac{dh_s}{dt} = SMB_s, \quad \text{with} \quad h_s \in \max(0, h_{s,\text{max}}). \quad (5)$$

If the snow height h_s exceeds a certain threshold $h_{s,\max}$ (here set to 5 mm) snow is transformed into ice—in a simple way resembling snow compaction:

$$\int_0^{\Delta t} C_{si} dt = \max(0, h_s - h_{s,\max}) \quad (6)$$

The described equations are solved using an explicit time-step scheme. ~~For faster computation we use with~~ a time step of 5 one day. In principle, the use of monthly input data is also supported but would require interpolation to daily time steps.

2.1 Surface heat fluxes

We describe the outgoing longwave radiation as a function of surface temperature according to the Stefan–Boltzmann law:

$$LW^\uparrow = \sigma T_s^4 \quad (7)$$

For the turbulent heat exchange (sensible and latent) we use a standard bulk formulation (e.g., [Gill, 1982](#)):

$$H_S = C_S \rho_a c_{p,a} u_s (T_s - T_a) \quad (8a)$$

$$H_L = C_L \rho_a L_s u_s (q_s - q_a) \quad (8b)$$

with sensible and latent heat exchange coefficients C_S and C_L , air density ρ_a , specific heat capacity of air $c_{p,a}$, surface wind speed u_s , air temperature T_a , latent heat of sublimation/deposition L_s , and air specific humidity q_a . ~~Air density ρ_a is not available from MAR and thus approximated by the ideal gas law $\rho_a = \frac{p}{R_s T_a}$, with specific gas constant $R_s = 258 \text{ J kg}^{-1} \text{ K}^{-1}$, and surface pressure p , which is available from MAR.~~ Specific humidity over the snow or ice surface (q_s) is assumed to be saturated and depends on surface pressure p_s and saturation water vapour pressure e^*

$$q_s = \frac{e^* \epsilon}{e^*(\epsilon - 1) + p_s}, \quad \text{where} \quad (9)$$

$$e^* = 611.2 \exp \left(a \frac{T_s - T_0}{T_b + T_s - T_0} \right)$$

with $\epsilon = 0.62197$, the ratio of the molar weights of water vapour and dry air, and coefficients a , T_b , which are prescribed for 20 vapour pressure over water ($a = 17.62$, $T_b = 243.12 \text{ KK}$) or ice/snow ($a = 22.46$, $T_b = 272.62 \text{ KK}$). T_0 denotes the freezing point of water, 273.15 KK . See, [Gill \(1982\)](#) for [more](#) details.

2.2 The diurnal cycle of thawing and freezing

Because we use daily time steps, processes on time scales shorter than one day cannot be resolved explicitly. Hence, we cannot explicitly account for the thawing during daytime and the freezing during nighttime which is quite usual for the melting season 25 on Greenland. The absorbed shortwave radiation, for example, can exhibit large diurnal variations, especially when the surface albedo is low (Cuffey and Paterson, 2010). During the day, near surface temperatures may rise above freezing temperature and

snow or ice starts to melt. During the night, temperatures drop below freezing and any liquid water such as previously melted water can refreeze within the snowpack.

To account for this process we introduce a [parametrisation-parameterisation](#) for the diurnal cycle of thawing and freezing. We simply assume a sinusoidal temperature curve $T(t)$ throughout the day (here, units of time t are hours h) around a given 5 mean surface temperature T_s (here, we refer to T_s with units in $^\circ\text{C}$) with amplitude A , i.e., a cosine function (Fig. 1a):

$$T(t) = T_s - A \cos\left(\frac{2\pi}{24}t\right) \quad (10)$$

For the sake of simplicity we use a single constant A , although in reality it is spatially and temporally dependent as shown in Fig. 1b.

Melting and refreezing may then occur on the same day if (potential, not actual) T_s exceeds 0°C . The amount of melting and 10 refreezing then depends on the amplitude A and the mean daily temperature T_s (Fig. 1a). Fortunately, an analytical solution to this problem exists. We calculate the roots of the cosine function and then integrate between the roots to solve for average above- and below-freezing mean surface temperatures T_s^+ and T_s^- . The roots are

$$t_1 = \frac{24}{2\pi} \arccos\left(\frac{T_s}{A}\right), \quad t_2 = 24 - t_1.$$

Thus, the time span for temperatures above and below freezing is

$$15 \quad \Delta t_+ = t_2 - t_1 = 24 - 2t_1, \quad \text{and} \quad \Delta t_- = 2t_1.$$

This leads us to an expression for averages of above- and below-freezing temperatures T_s^+ and T_s^- . These are the integrals of the cosine function

$$T_s^+ = \frac{1}{\Delta t_+} \int_{t_1}^{t_2} T(t) dt \quad (11a)$$

$$20 \quad T_s^- = \frac{1}{\Delta t_-} \int_0^{t_1} T(t) dt + \int_{t_2}^{24} T(t) dt \quad (11b)$$

$$= \frac{24}{\pi \Delta t_-} \left[T_s \arccos\left(\frac{T_s}{A}\right) - A \sqrt{1 - \frac{T_s^2}{A^2}} + \pi T_s \right]$$

This parameterisation depends on the prescribed diurnal cycle amplitude, A , which affects the amount of melting and refreezing and, thus, the surface mass balance. Note, melt energy Q_m and “cold content” Q_c in the following Eq. (12) are 25 calculated by using T_s^+ and T_s^- , respectively. Without this [parametrisation-parameterisation](#) or with A set to zero, melting and refreezing cannot occur at the same time step and instead, the actual surface temperature T_s must be used.

2.3 Melting and refreezing

Additional processes that affect the snowpack temperature are melting and refreezing. During ~~24 h~~ ~~the course of one day~~ ~~the~~ energy available for melt Q_m and refreezing (the so-called “cold content”) Q_c are defined as

$$Q_m = \begin{cases} (T_s^+ - T_0) \frac{c_{\text{eff}}}{\Delta t} & \text{if } T_s^+ > T_0, \\ 0 & \text{if } T_s^+ \leq T_0, \end{cases} \quad (12a)$$

5 and

$$Q_c = \begin{cases} 0 & \text{if } T_s^- \geq T_0, \\ (T_0 - T_s^-) \frac{c_{\text{eff}}}{\Delta t} & \text{if } T_s^- < T_0. \end{cases} \quad (12b)$$

Thus, the potential melt is

$$M_{\text{pot}} = \frac{Q_m}{\rho_w L_m} \quad (13)$$

with ~~water density~~ ρ_w , latent heat of melting (or fusion) L_m , and time step Δt . Actual melt depends on how much ~~solid water~~,

10 ~~i.e.~~ snow or ice ~~,~~ is available for melt. If potential melt is larger than the current snow height all snow melts down and the excess melt energy is used to melt the underlying ice. Ice-free land is treated differently and the excess melt energy is used to warm the surface. The actual melt M is then the sum of melted snow and melted ice:~~;~~

$$M_{\text{snow}} = \min(M_{\text{pot}}, h_s / \Delta t) \quad (14a)$$

$$M_{\text{ice}} = M_{\text{pot}} - M_{\text{snow}} \quad (14b)$$

15 $M = M_{\text{snow}} + M_{\text{ice}} \quad (14c)$

The refreezing rate depends on the potential liquid water to be refrozen, i.e., the actual melt rate M and rainfall P_r . Analogous to the melt rates, the potential refreezing is given by

$$R_{\text{pot}} = \frac{Q_c}{\rho_w L_m}. \quad (15)$$

Suppose some ~~liquid water, i.e.,~~ rain or melt water ~~,~~ exists within the snow pack. The “cold content” Q_c is then used to 20 (virtually) turn ~~this~~ liquid water into frozen water, i.e., snow or ice. We distinguish between refrozen rain and refrozen melt water

$$R_{\text{pot,rain}} = \min(R_{\text{pot}}, P_r) \quad (16a)$$

$$R_{\text{pot,melt}} = \min(\max(R_{\text{pot}} - R_{\text{pot,rain}}, 0), M_{\text{snow}}) \quad (16b)$$

$$R = R_{\text{rain}} + R_{\text{melt}} = \underline{f_R} (R_{\text{pot,rain}} + R_{\text{pot,melt}}) \quad (16c)$$

25 ~~We Because of its porous structure the snowpack retains a limited amount of melt water and this melt water retention is reflected by the refreezing correction parameter f_R which acts on the potential refreezing of rain and melt water. In contrast, ice itself~~

does not retain any melt water at the surface, so we assume that it has a water holding capacity of zero. We can therefore neglect refreezing of melted ice and treat ice melt as runoff.

As noted in the beginning of this section, melting consumes internal energy of the snowpack, while refreezing releases internal energy. SEMIC accounts for both melting and refreezing, and therefore the associated temperature change in Eq. (1) 5 via $Q_{M/R}$ —the residual energy for refreezing or melting—:

$$Q_{M/R} = \rho_w L_m (M - R) \quad (17)$$

Here, we see how tightly the mass balance and the energy balance are coupled and that great care must be taken when the underlying surface processes are incorporated into one model.

2.4 Snow albedo parameterisation

10 We use a modified version of an albedo parametrisation for snow simple surface albedo parameterisation that depends on snow temperature (Slater et al., 1998). The original version describes albedos for the near-infrared and the visible band. Because the dependence on temperature of both albedo terms are similar, we combined these two into one albedo term.

15 The reasoning of a temperature-dependent snow albedo is as follows: Albedo declines if snow starts to melt and melting is much more likely for higher temperatures. The snow albedo above a certain temperature threshold, here T_{min} , is temperature dependent and starts to decline to the snow albedo of old snow, i.e., $\alpha_{s,min}$ as temperatures approach the melting point T_0 . Below the temperature threshold T_{min} , we assume that snow does not change and has an albedo of fresh snow, i.e. $\alpha_{s,max}$. The relationship between snow albedo and temperature can, therefore, be described according to

$$\underline{\alpha_s} = \alpha_{s,max} - (\alpha_{s,max} - \alpha_{s,min}) t_m^3 \quad \text{with}$$

$$\underline{t_m} = \begin{cases} 0 & \text{if } T_s < T_0, \\ \frac{T_s - T_{min}}{T_0 - T_{min}} & \text{if } T_{min} \leq T_s < T_0, \\ 1 & \text{if } T_s > T_0. \end{cases}$$

20 T_{min} is set to 263.15 K as originally proposed (Slater et al., 1998).

The actual, the background albedo, and the snow height (Oerlemans and Knap, 1998). The surface albedo α is then defined as is the average of fresh snow albedo α_s and the prescribed background albedo α_i for ice-covered or α_l for ice-free land and depends on the critical snow height h_{crit}

$$\alpha = \alpha_s - \underline{f_a} \exp \left(\frac{-h_s}{h_{crit}} \right) (\alpha_s - \alpha_{bg}) \quad \text{where} \quad \alpha_{bg} = \begin{cases} \alpha_i & \text{for ice-covered or} \\ \alpha_l & \text{for ice-free land} \end{cases} \quad \underline{\text{and } f_a = \exp(-h_s/h_{crit})}. \quad (18)$$

25 Although the snow albedo depends on temperature only, the grid-averaged albedo includes snow height as well as the characteristics of the underlying surface (i.e., ice or bare land), thus providing enough degrees of freedom to capture the variety of surface conditions over ice- and snow-covered regions. We also compared our approach to a more sophisticated albedo parameterisation

that includes a temperature-dependent snow albedo (Slater et al., 1998) but concluded that the added value is too little given the reduction in model performance.

2.5 Boundary conditions, initial conditions, and model performance Model Setup

To drive the model we need as input: incoming short- and longwave radiation, near-surface air temperature, surface wind speed, near-surface specific humidity, surface pressure, snowfall, and rainfall, either computed by ~~an~~¹ a coupled atmosphere model or prescribed as atmospheric forcing. For example, these fields can also be obtained from an interactive coupling to an atmospheric model. In order to evaluate the model, we choose to run the model offline using prescribed atmospheric forcing. Forcing fields are listed in Table 2.

In this paper, we use daily mean data from the regional climate model MAR, version 2 (Fettweis et al., 2013), which includes the multi-layer snowpack model SISVAT (Soil Ice Snow Vegetation Atmosphere Transfer), to tune and optimise our model parameters. At its lateral boundaries MAR is forced by the general circulation model CanESM2 under historical conditions and under the global warming scenario RCP 8.5 (for details, see Fettweis et al., 2013). As input to SEMIC, we use the output of the last three model years of MAR output from the historical period, i.e., 10 years from 1990–1999, and from the 21st century scenario RCP8.5, i.e., 2098–2100, because they are representative of more extreme climatic 10 years from 2090–2099, as these periods represent present-day climate and future extreme warming conditions for the Greenland ice sheet. First, its associated surface mass balance exhibits the strongest seasonal variability at the end of the 21st century in RCP8.5. And second, because those three years also capture substantial year-to-year variability. The well.

To reduce the large amount of forcing data for the whole 20 years, we simply use a random sub-sample accounting for 25% of land and ice points. The overall memory demand for the calibration procedure is thus reduced by a factor of about 10. For each new initialisation, the model requires several years of spinup—especially spin-up—especially the snow pack height h_s and hence the associated surface albedo α (see Eq. 18) responds rather slowly. We refrain to use more than three years because of the expected larger computational overhead¹, which likely increases the overall computation time given that several thousands of calibration iterations are to be expected. Therefore, we loop 20 times over those three years 10 times over each of the 10-year periods to advance the variables from their initial conditions. The last iteration over the three years output from the last iteration, i.e., the final 10 years, is then used for the comparison with MAR output.

Our current setup is designed to allow testing and tuning of the snowpack model driven by prescribed atmospheric forcing. Thus feedbacks with the atmosphere via near-surface heat fluxes are currently not active, reducing the degrees of freedom of the model. It is important to remember that while SEMIC is driven by atmospheric forcing from MAR, the main comparison is with MAR’s snowpack model SISVAT although SEMIC calculates several surface-atmosphere heat fluxes such latent heat, sensible heat, and upward longwave radiation as done by MAR. But for the sake of clarity, from now on we refer to MAR whenever a comparison between SEMIC and MAR/SISVAT output is being made.

On a modern laptop (e.g., MacBook Pro with an Intel Core i7, 2.8 GHz), 100 years of integration with daily time steps on a grid with 6,720 points (i.e., the MAR grid with 25 km horizontal resolution) take about 40 seconds for SEMIC. Of course, in

¹Three years of MAR data amounts already to 3.7Gb.

coupled and stand-alone applications there is overhead for exchanging the variables and writing the output, thus, adding to the overall computation time. However, SEMIC is a fast model and therefore well suited for multi-millennial integration such as glacial cycles.

3 Model parameter calibration

5 To calibrate our free model parameters we minimise errors with respect to MAR output. Afterwards the optimised parameters are used to compare SEMIC with results for the whole historical period from 1970–2005 and for the warming scenario RCP 8.5 from 2006–2100. The periods 1990–1999 and 2090–2099 represent a subset, i.e., a training data set of the historical period and the RCP8.5 scenario.

At the model initialisation, T_s and α_s are prescribed with values from MAR output of the first days, i.e., Jan 1 2098 10 and we set $h_s = 1\text{ m}$ 1990 and 2090. Because we do not know the water equivalent snow height from MAR and we initially set $h_s = 1\text{ m}$. After a few time steps the fast responding variables T_s and α_s are close to their expected trajectories. However, response time for h_s is much longer and difficult to quantify because it depends on the slowly varying and highly sensitive mass balance terms. Therefore, several years of integration can be necessary for the model spinupspin-up. To account for the longer response time of h_s we loop 2010 times over the three years, 2098–210010 years, 1990–1999 and 2090–2099, creating 15 an effective integration period of 60100 years. From those 2010 loops, the last iteration, i.e., the last loop– final loop over the 10 years is used to estimate the error between SEMIC and MAR. The model initialisation and spinup– spin-up is done every time SEMIC uses a new model parameter set, in order to treat each of those parameter settings in a comparable way.

The quality of our parameters is measured with the normalised centred root mean square error E . It is a good way to estimate how closely a test field (SEMIC output in our case) resembles a reference field (MAR output) in terms of correlation 20 and variance (Taylor, 2001) while also allowing to assessthe assessment of variables with different units:

$$E = \sqrt{\frac{1}{N} \sum_{n=1}^N \left[\frac{(X_n - \bar{X}) - (Y_n - \bar{Y})}{\sigma_Y} \right]^2 + [\sigma_X/\sigma_Y - 1]^2} \sqrt{\frac{1}{N} \sum_{n=1}^N \left[\frac{(X_n - \bar{X}) - (Y_n - \bar{Y})}{\sigma_Y} \right]^2 + \left[\frac{\bar{X} - \bar{Y}}{\sigma_Y} \right]^2} \quad (19)$$

Here, X is some SEMIC time series with N time steps. This could be any model variable, for example, averaged surface temperature T_s , net shortwave radiation $SW_{net} = (1 - \alpha)SW^\downarrow$, or surface mass balance $SMB = P_s - SU - M + R$. The symbol Y represents the corresponding MAR time series and the σ 's are the standard deviations of the time series. Overbars 25 denote temporal averages of the time series.

3.1 Minimising the cost function

To include Greenland's diverse climate zones, we choose the time series (i.e., the X_n 's and Y_n 's) as being spatial averages over ice-free land and over three different ice-covered regions, all shown in Fig. 2. The three ice-covered regions crudely represent the main ablation zones at the ice-sheet margins (region 1), the main accumulation zone at ice-sheet interior (region 3), and a 30 mixed zone in between the main accumulation and ablation zones (region 2). We thereforeNote, the outlined regions represent

different mass balance zones for today's climate and may change for any future warming scenario such as RCP8.5. Still, the distinction is useful to derive a differentiated response in each of those regions to the atmospheric forcing. We calculate four different E values, one over ice-free land (E_L) and three over the different ice-covered regions (E_{b1}, E_{b2}, E_{b3}) for both periods, 1990–1999 and 2090–2099, denoted by a subscript, e.g., E_L^{hist} or E_{b2}^{rcp85} .

5 For our cost function we regard the following variables as important for the surface energy and mass balance: surface temperature T_s , net shortwave radiation SW_{net} , cumulative melt M_{cum} , and cumulative melt M , and surface mass balance SMB_{cum} . The magnitude of this vector then defines our cost function J

$$J = \left\| \left(E_{L,T_s}^{hist}, E_{b1,T_s}^{hist}, \dots, E_{L,SW_{net}}^{hist}, \dots, E_{b3,SMB_{cum}}^{hist}, E_{L,T_s}^{rcp85}, \dots, E_{b3,SMB}^{rcp85} \right)^T \right\| \quad (20)$$

which we want to minimise. Note that we assign different area weights to each of the regions based on their area.

10 The cost function J is minimised with a method called *Particle Swarm Optimisation*, described below. Using these calibration steps, we derive these optimal parameters values: $A = 3.4 \text{ K}$, $\alpha_{s,\min} = 0.77$, $\alpha_{s,\max} = 0.79$, $\alpha_i = 0.80$, and 0.41 , $\alpha_l = 0.07$, $h_{\text{crit}} = 0.090.028 \text{ m}\cdot\text{m}$, and $f_R = 0.85$ which are also listed in Table 3.

3.2 Particle Swarm Optimisation

Because of the high dimensionality of the parameter space, a random search for the optimal parameters would need a large sample size in the order of $\mathcal{O}(10^{5-6})$. One optimisation technique that overcomes the problem of large sample sizes is the so-called *Particle Swarm Optimisation* (PSO) (Poli et al., 2007). PSO is based on social interaction among particles of the 'swarm'. Initially, each particle is placed randomly in the parameter space and has a random velocity. For all particles the cost function J is calculated (Eq. (20)). This determines the "fitness" of each individual and of the swarm as a whole. Now, each particle updates its current position and velocity in the parameter space depending on its current and current-best fitness position, and also on the global best-fitness position, with some random perturbations. The next iteration starts after all particles have moved. Eventually, the swarm as a whole moves to the minimum of the cost function J . For our parameter calibration we let 30 particles freely swarm within the four-dimensional parameter space. The global best-fitness solution found within 100 iterations¹ is then regarded as optimal.

3.3 Calibration results

25 The ice-sheet surface temperature is very well constrained by the atmospheric forcing fields. Therefore, the surface temperature in SEMIC is similar to the one calculated by MAR, as the annual mean differences and the ice-sheet averaged time series show (Fig. ?? and ?? Figs. 3, 4, 5, and 6). The annual mean difference between SEMIC and MAR is about -0.2 for years 1990–1999 (2090–2099) is about 0.4 K (0.3 K) over the ice sheet and -0.20.5 K (0.2 K) over ice-free land. While large parts of the ice sheet are slightly colder in SEMIC, temperatures at the ice divides are slightly and over ice-free land are generally warmer in 30 SEMIC (see Fig. ?? Figs. 3i and 4i).

¹Note, 100 iterations are a pre-defined upper limit and usually solutions tend to converge earlier.

The surface mass balance is also well captured by SEMIC. The largest differences occur in the ablation zones of region 1 and 2 around the margin of the ice sheet. While melting² over the northern part of the ice sheet is overestimated by SEMIC, it is underestimated over the southern part of the ice sheet. Nonetheless, for years 1990–1999 (2090–2099) the overall surface mass balance difference over the ice sheet between SEMIC and MAR is 0.13 almost zero, -0.04 (-0.03) mm/day mm day⁻¹, with SEMIC having an average surface mass balance of -1.381.57 (-0.24) mm/day (-1.51 mm day⁻¹, and 1.61 (-0.21) mm/day in MAR). The relative difference between mm day⁻¹ in MAR. SEMIC and MAR is about 9% over the whole ice sheet. also exhibit similar melt rates over the ice sheet with differences of -0.06 (-0.15) mm day⁻¹. A detailed overview of the differences from the model variables that we used to define the cost function is provided in Table 4.

In regions where surface mass balance is positive (see Fig. 3c and g and 4c and g), errors are small because accumulation is mainly prescribed by snowfall and to a lesser extent by sublimation/evaporation. Therefore, differences in ablation are more important because they arise dynamically from SEMIC. The introduced diurnal cycle parameterisation is critical here; it allows melting and refreezing within one time step which would be prohibited otherwise.

SEMIC produces less melt than MAR by 0.11 mm per day, with an average annual ice sheet melt rate of 3.38 mm per day, which corresponds to a relative difference of about 5% compared to MAR. This is a result of more refreezing and larger sublimation rates in the ablation zone of the ice sheet.

SEMIC is able to capture both, the increase and decrease of surface mass balance as well as the seasonal melting as shown for the different regions in Fig. 7 and periods in Figs. 5 and 6. As can be seen from Fig. 7, errors in melt rates and the surface mass balance accumulate over time. Particularly, over land and around the ice sheet margin (region 1 and partly region 2). The calibration procedure minimises discrepancies across the four regions and across the two different calibration periods. This results in melt rates that are slightly too large in all regions and for both periods but the surface mass balance is slightly too large. This will have an effect on itself is reasonably well modelled by SEMIC except for the inner ice sheet region 3 for the years 2090–2099. Overall, using the resulting optimal parameters from the calibration improves SEMIC's performance for the historical simulation and for RCP 8.5 (2005–2100) in modelling the whole historical and RCP8.5 period from 1970–2099 as shown in the next Sect. 4.

The Taylor diagram in Fig. 9 summarises the performance of SEMIC compared to MAR and its multi-layer snowpack model. Except the surface mass balance for the RCP8.5 years and the melt for the historical period in the interior of the Greenland ice sheet (region 3), all variables are reasonably close to the reference value of each regions' time series in terms of their variability, measured via their standard deviation and their match to the corresponding MAR variables, measured via their correlation. A detailed look into each time series (Fig. 5 and 6) further supports our results that SEMIC and MAR variables are reasonably close to each other, especially during the whole melt season.

We find that the overall differences between SEMIC and MAR temperature and surface mass balance are reasonably small given the challenge of i) matching both periods, 1990–1999 and 2090–2099, ii) calibrating different mass and energy balance variables in parallel, and iii) using only a subset of grid points (25%) averaged over four regions across entire Greenland. SEMIC's annual mean values of surface temperature and surface mass balance are well suited for applications of

²Note that melt is defined here as a positive quantity but is subtracted from the surface mass balance.

interactive ice sheet models. The optimisation guarantees that the regionally averaged MAR and SEMIC time series are as close as possible (as defined by the cost function). Still, SEMIC is sensitive to the choice of parameters. ~~Next we, so we now~~ show how perturbed parameters around their optimal values affect the surface energy and mass balance of the ice sheet.

3.4 Parameter Sensitivity

5 We identified parameters that dominate model uncertainties and tested the parameter sensitivity on the model performance (e.g., Fitzgerald et al., 2012). We addressed the sensitivity of ~~each SEMIC parameter~~ ~~the SEMIC model parameters~~ listed in Table 3 (Fig. 8). ~~Therefore, we varied by varying~~ each parameter freely while keeping the others ~~fixed~~ at their optimal value. In this way, we estimated the contribution of each individual parameter on the cost function J . ~~The effect of parameter variations on the individual cost function for surface temperature T_s , surface mass balance SMB , surface melt, shortwave radiation SW_{net} is also calculated because each variable responds differently to different model parameters.~~

10 ~~SW_{net} is also calculated because each variable responds differently to different model parameters.~~

As can be seen for all parameter sensitivity graphs in Fig. 8, the Particle Swarm Optimisation was able to find ~~the optimal value for each parameter, i.e., an optimal parameter set for which the~~ PSO minimises J . Therefore, we are confident that this optimal parameters set provides us with a globally optimised model setup.

15 The ~~sensitivity to~~ cost function shows a large sensitivity to variations of the diurnal cycle amplitude A ~~is largest for melting because~~ and the fresh-snow albedo α_s . The sensitivity to the other albedo-relevant parameters, that is α_i , α_l , and h_{crit} ~~is rather small. The diurnal cycle and thus~~ A ~~directly defines the magnitude of daily melt rates. If~~ A ~~is too low, melt would be underestimated in SEMIC compared to MAR; and vice versa for too large~~ A . ~~However,~~ ~~directly affect melt and the surface mass balance itself is less sensitive. The local minimum of the cost function for~~ A ~~than melting. The reason is that even if melting would be enhanced or suppressed, refreezing would almost compensate for that because it depends on the available meltwater.~~ ~~is also in line with the range of diurnal cycle amplitude values around the ablation zone of the Greenland ice sheet, as is modelled by MAR during summer (Fig. 1b).~~

20 ~~The sensitivity to the maximum snow albedo $\alpha_{s,max}$ is, as to be expected, largest for the net shortwave radiation because it directly limits the amount of radiation absorbed in the snowpack. Melting is also sensitive to the amount of shortwave radiation entering the snowpack. If more energy is available to raise the snowpack temperature the likelihood for melting is of course larger as well. Melt is also sensitive to changes in the minimum snow albedo $\alpha_{s,min}$ but the surface mass balance exhibits an extraordinarily larger sensitivity.~~

25 ~~Almost all cost functions show a sensitivity to variations of critical snow height. The parameter α_s directly affects the radiation budget, where a small percent change makes a large difference in terms of receiving short-wave radiation. The cost function is less sensitive to the other albedo parameters. Values of h_{crit} . As before, the surface mass balance shows the largest sensitivity to changes in h_{crit} . Because h_{crit} determines how much weight we put on the snow albedo or the background albedo, i.e., bare ice or land albedo, it directly influences how much shortwave radiation is absorbed below 2 cm or above 5 cm would lead to non-optimal solutions because it dictates how much ice and how much snow can be "seen" by short-wave radiation and, in this way, influences the surface energy balance.~~

The parameter sensitivities reveal that our previously calibrated parameters are close to the calculated local minima for each of the individual cost functions optimal refreezing correction parameter f_R is 0.85 (see Table 3). This large proportion of melt water refreezing underlines the importance of the refreezing process in determining the surface mass balance of the Greenland ice sheet. Any lower refreezing correction leads to a less optimal cost function.

Having determined the optimal parameter set we can now compare SEMIC with MAR for the whole historical and RCP8.5 period from 1970–2100.

4 Model validation

As a final step of the full model analysis, we use the optimised model parameters for the following two model validation runs: a) A historical run from 1970–2005 and b) an RCP8.5 scenario run from 2006–2100³. This time, we compare SEMIC with MAR for a whole time series instead of just a few years as done for the calibration. We take a closer look into the regional differences of surface temperature, surface melt, and surface mass balance over the four previously defined regions and calculate the corresponding time series of their annual mean values, as shown in Fig. 10.

Annual mean surface temperatures correspond well with MAR results and both time series are hard to distinguish from each other. To a lesser extent but still reasonably well, surface melt and surface mass balance are captured by SEMIC. The decline of surface mass balance throughout the 21st century in the RCP8.5 scenario is evident over the three ice-sheet regions, while the mass balance remains close to zero over ice-free land. Furthermore, SEMIC captures the year-to-year variations throughout the historical and the RCP8.5 period. This tells us that the newly introduced diurnal cycle parameterisation makes SEMIC more realistic and thus comparable to more comprehensive and complex multi-layer snowpack models. We believe that a representation of the diurnal thawing and freezing cycle is essential for SEMIC and for physically correct mass balance modelling in general, and thus represent an important advance.

The overall performance of SEMIC with respect to the more sophisticated regional climate model MAR is satisfactory, given its intended use for long time-scale simulations. In the validation test we show that SEMIC is able to capture long-term trends of the Greenland ice sheet under the RCP8.5 scenario, while also reproducing the interannual variability exhibited by MAR.

5 Discussion

In this paper we use output from MARv2 forced by CanESM2 as described in Franco et al. (2013) for the simple reason that Xavier Fettweis made the full daily MAR output data publicly available (see below in Sect. 7). Unfortunately, version 2 of the MAR model is outdated and superseded by MARv3.5.2 (Fettweis et al., 2016) and subsequently the surface mass balance estimates of SEMIC are also not up to date and care should be taken to interpret these results in the light of future climate change. The main point and purpose of this study is that SEMIC reasonably well represents the surface mass balance as modelled by MARv2. In principle, SEMIC could be applied to any type of data, for example, to output from other regional

³Data is available at

climate models such as RACMO (Noël et al., 2015), to re-analysis data such as ERA-Interim (Dee et al., 2011), or even to in-situ observational data sets such as PROMICE (van As et al., 2016). A preliminary analysis (which is beyond the scope of this study) using meteorological data from Col de Porte (Morin et al., 2012) suggests that SEMIC is also capable to reproduce reasonable results when forced by observational data.

5 The definition of a cost function for the model calibration is a non-trivial task. SEMIC computes several variables which, in principle, could all be included in the cost function. We choose to take into account, first, the net shortwave radiation which is determined by the albedo ~~parametrisation~~ ~~parameterisation~~ and its parameters and which in turn determines surface temperatures. Second and third, the surface mass balance and the surface temperature are considered, in anticipation of the interactive coupling to an ice-sheet model. And fourth, melting to account for the newly introduced diurnal cycle parameterisation of
10 thawing and freezing. Still, it is clear that the choice of the cost function and the variables considered is subjective.

In the model calibration and validation we weighted each of the regions on the area. The area of the ice-free land and region 1, for example, is nearly as large as either region 2 or 3. Consequently, the influence of the smaller regions—here, land and region 1—is much smaller than that of the larger ones, such as regions 2 or 3, despite region 1 being a major driver of surface melting.

15 For the calibration of model parameters, we ~~explicitly chose the last three years, 2098–2100, of the chose ten years at the end~~
~~20th century, i.e., years 1990–1999 from the historical period and ten years at the end of the 21st century, i.e., years 2090–2099~~
~~from the~~ RCP8.5 scenario ~~because those years exhibit the largest year-to-year variability as well as the largest surface melt~~
~~rates/lowest mass balance rates for the available period from 1970–2100 (see Fig. 10). Pushing SEMIC to its limits in terms of~~
~~forcing it with the most~~. Those years cover periods of moderate melt under present-day climate conditions and more extreme
20 melt under a strong warming scenario. Forcing SEMIC with both moderate and extreme climate conditions ~~on record, is good~~
~~evidence shows~~ that our model ~~can also represent less extreme climate conditions, such as, for example, the historical period~~
~~or other any other RCP scenario~~ is capable of representing the surface energy and mass balance of the Greenland ice sheet under
~~different climate conditions and is thus very well suited for future and past climate studies such as glacial cycles.~~

There are two main reasons why surface temperature is better represented in SEMIC than the surface mass balance: 1)
25 Surface temperature is determined by the driving atmospheric processes, which in our case are prescribed by MAR atmospheric forcing. Therefore changes in the atmosphere are directly reflected at the surface in terms of energy balance. 2) Surface mass balance is harder to constrain because the processes within the snowpack are more complex. Mass can be added by the atmosphere via rain and snowfall, and mass can be removed via melting. Within the snowpack melted water can refreeze if the temperature allows that. Refreezing depends on the available liquid water, i.e., rain or melted ice/snow, and on the energy
30 budget, i.e., the “cold content”. The multitude of feedbacks involved in the surface mass balance makes it far less constrained by external forcing variables than surface temperature.

We only describe the large-scale effects of changes in the snowpack and we omit a microscopic description of snow physics (e.g., Vionnet et al., 2012). SEMIC can therefore be thought of as a surrogate of a more complex multi-layer snowpack model. We have developed SEMIC as a coupler between interactive ice sheet models and EMICs (Earth-System Models of
35 Intermediate Complexity) or coarse resolution GCMs (General Circulation Models). SEMIC realistically represents the energy

transfer between atmosphere and surface as radiation and turbulent mixing of heat and water vapour, thus providing a general solution to the surface energy balance that is applicable for different climates and time scales.

Ice-free land and ice-covered land are treated differently in SEMIC because of the different physical processes involved. For example, the surface temperature of ice- and snow-free land has no upper limit as is the case for surface temperatures of ice, 5 which is always lower than or equal to the freezing point. Generally, land albedo is much more variable than as described by the single bare land albedo used in SEMIC. Different land and vegetation types have different effects on the radiation budget. Consequently, net shortwave radiation errors in SEMIC are larger over ice-free land than over the ice sheet (Fig. ??[Figs. 3j and 4j](#)).

Details in model representation also reveal differences between SEMIC and MAR. However, these differences are not so 10 much related to the underlying physical principles, i.e., the assumption of energy and mass balance of the snow- and ice-covered surface, as to the choice of parameters made in order to match SEMIC variables to MAR variables.

SEMIC makes use of two simple but effective parameterisations that are important for its good performance: One is the surface albedo for which we already discussed the problem of the net shortwave radiation budget over ice-free land. Although the net shortwave radiation has an effect on the surface energy balance, errors do not translate directly into errors in the surface 15 temperature (Fig. ??[Figs. 3i and 4i](#)). One reason is that the contribution of sensible and latent heat flux is larger over ice-free land because of the larger temperature contrast. Latent heat flux, for example, is about 10 times larger over ice-free land than over the ice sheet.

Another reason for SEMIC's good performance is the [diurnal cycle parameterisation](#) [newly introduced diurnal cycle parameterisation](#), which allows for faster computation while adding the daily thaw–freeze cycle during melt season. The representation of the 20 diurnal cycle of the whole ice sheet by a single constant value is somewhat problematic because in reality, it changes over time and location, depending on the climatic conditions, e.g., cloud cover and its effect on downwelling longwave radiation. Still, the overall results of SEMIC with respect to surface mass balance are satisfactory. The diurnal cycle opens many new aspects which could improve model results, e.g., a spatial dependence such as height-dependent amplitude or a direct calculation of the amplitude by the coupled atmospheric model, but this is beyond the scope of this paper. Also, a different or a more realistic albedo scheme could replace the current [simple albedo parameterisation \(Oerlemans and Knap, 1998\)](#). SEMIC has also 25 [been successfully tested with a](#) [temperature-dependent implementation based on the work by Slater et al. \(1998\)](#) [albedo scheme](#) (Slater et al., 1998), for example.

Our results underpin the consistent representation of the dominant processes involved in the complex interactions between snow- or ice-covered surfaces and the atmosphere. SEMIC incorporates simpler dynamics compared to multi-layer snowpack 30 models, but represents the essential surface energy and mass balance processes, and is still fast in terms of computational time.

SEMIC is well suited for long-term integrations up to several millennia and has been successfully tested for the last 78,000 years (data taken from Heinemann et al., 2014, personal communication). From the 100 year run-time estimate we can assume that computation of the surface mass balance on every single day during one glacial cycle (of about 100 k years) would take about 11 h. Current state-of-the-art multi-layer snowpack models are not able to perform such long integrations but they also 35 do not serve this purpose. Under these circumstances, using a much simpler model—such as SEMIC—is advised.

SEMIC is well suited for applications with global climate models which have just started to master glacial time scales (e.g., Heinemann et al., 2014). SEMIC will be part of the next version of the regional energy and moisture and balance model REMBO (Robinson et al., 2010) and is also ready to be coupled to an interactive ice-sheet model. SEMIC is considered as an open-source project, therefore contributions are welcome, and we encourage and support the integration of SEMIC into [climate](#) and ice-sheet models.

6 Conclusions

6 Conclusions

We have presented a new Surface Energy and Mass balance model of *Intermediate Complexity* (SEMIC) for snow- and ice-covered surfaces that is simple and fast enough for long-term integrations up to glacial time scales. SEMIC is a physically based model that accounts for energy and mass balance and it can be used as a surrogate for computationally intensive regional climate models with their multi-layer snowpack models. The most important features of SEMIC are a simple but effective surface albedo parameterisation and a [parametrisation](#) of the daily thaw-freeze cycle that allows partitioning between melting and refreezing. [Compared to the more sophisticated SEMIC has been forced with atmospheric fields from the regional climate model MAR \(MARv2\) and compared to MAR's multi-layer snowpack model SISVAT](#), SEMIC represents surface temperature and surface mass balance considerably well. [SEMIC matches climatological trends, e.g., For the RCP8.5 warming scenario, while preserving realistic interannual variability. If SEMIC correctly simulates the climatological trend and the interannual variability of surface temperature and the mass balance of the ice sheet. SEMIC hereby](#) incorporates a minimum number of free model parameters and a large effort was made to balance the complexity of the represented processes in favour of faster computation.

20 7 Scientific Reproducibility, Transparency, and Data Availability

We hereby acknowledge, support, and encourage research that follows standards with respect to scientific reproducibility, transparency, and data availability. Any model source code and the authors' manuscript source (typeset in \LaTeX) is freely available and accessible online.

The project infrastructure covering individuals step starting from data download and preparation, model source code compilation, running the optimisation, running the calibrated model, running the model with historical and RCP8.5 scenario data, as well as the source code of this manuscript with its figures can be downloaded from the repository website <https://gitlab.pik-potsdam.de/krapp/semic-project>. See the project website's `README.md` for details. The project can also be cloned using `git`:

```
git clone -b v1.1 git@gitlab.pik-potsdam.de:krapp/semic-project.git
```

The atmospheric forcing data from the MAR/CanESM2 model for the historical period from 1970–2005 and for the RCP8.5 scenario for the period from 2005–2100 are available at <ftp://ftp.climato.be/fettweis/MARv2/>.

Author contributions. M.K., A.R., and A.G. designed the model. M.K. implemented the model code with contributions from A.R.. M.K. implemented and carried out the model calibration and the data analysis. M.K. prepared the manuscript with contributions from all co-
5 authors.

Competing interests. The authors declare that they have no conflict of interest.

Acknowledgements. We would like to thank Xavier Fettweis for providing MAR/CanESM2 data. M.K. is also grateful to Malte Heinemann and Axel Timmermann for their kind hospitality during his research visit at the *International Pacific Research Center* (SOEST, University of Hawaii). A.R. was funded by the Marie Curie 7th Framework Programme (Project PIEF-GA-2012-331835, EURICE). M.K. was funded by
10 the Deutsche Forschungsgemeinschaft (DFG) Project "Modeling the Greenland ice sheet response to climate change on different timescales".

symbol

A 0.0–5.0 **3.1** amplitude of diurnal cycle (in K) $\alpha_{s,\max}$ 0.78–0.90 **0.80** maximum snow albedo, i.e., fresh dry snow $\alpha_{s,\min}$ 0.60–0.78 **0.77** minimum snow

c_{eff}

C_S

C_L

$c_{p,a}$

σ

T_0

ρ_w

L_s

L_v

L_m

T_{\min} 263.15 K minimum temperature threshold for albedo parametrisation $h_{s,\max}$

α_t 0.45 bare ice albedo, i.e., clean or blue ice α_t 0.15 bare land albedo height

Table 1. Model constants and their description.

symbol	description
SW^\downarrow	downwelling shortwave radiation (in-W m ⁻²)[W m ⁻²]
LW^\downarrow	downwelling longwave radiation (in-W m ⁻²)[W m ⁻²]
ρ_a	air density (in-kg m ⁻³)[kg m ⁻³]
u_s	surface wind speed (in-m s ⁻¹)[m s ⁻¹]
T_a	near-surface air temperature (in-K)[K]
q_a	near-surface specific humidity (in-kg kg ⁻¹)[kg kg ⁻¹]
p_s	surface pressure (in-Pa)[Pa]
P_s	snowfall rate (in-m s ⁻¹)[m s ⁻¹]
P_r	rainfall rate (in-m s ⁻¹)[m s ⁻¹]

Table 2. Atmospheric forcing fields needed as input for this model.

<u>symbol</u>	<u>range</u>	<u>value</u>	<u>description</u>
\underline{A}	0.0–5.0	3.0	amplitude of diurnal cycle [K]
$\underline{\alpha_s}$	0.70–0.90	0.79	fresh dry snow albedo
$\underline{\alpha_i}$	0.25–0.55	0.41	bare ice albedo, i.e., clean or blue ice
$\underline{\alpha_l}$	0.05–0.35	0.07	bare land albedo
$\underline{h}_{\text{crit}}$	0.00–0.20	0.028	critical snow height for albedo parameterisation [m]
$\underline{f_R}$	0.0–1.0	0.85	refreezing correction

Table 3. Model parameters with their initial range and their optimal value in bold face.

Table 4. Comparison of SEMIC and MAR. Shown are multi-year mean averages over the ice sheet (regions 1–3) and ice-free land, their mean gridpoint-to-gridpoint differences $\bar{\Delta}$, their minimum, and their maximum gridpoint-to-gridpoint differences, $\min \Delta$ and $\max \Delta$. Here, ice sheet means all ice-covered regions (region 1–3).

		1990–1999					2090–2099		
		SEMIC	MAR	$\bar{\Delta}$	$\min \Delta$	$\max \Delta$	SEMIC	MAR	$\bar{\Delta}$
ice sheet	T_s (in K) [K]	255.6 249.6	255.4 249.2	-0.2 1.4	-0.7 0.2	2.7 4.8	256.1	255.8	1.3
	SW_{net} (in W/m ²) SMB [mm day ⁻¹]	30.6 1.57	31.3 1.61	-0.7 0.96	-9.6 1.78	7.7 2.88	-0.24	-0.21	0.97
	SMB (in mm/day) M [mm day ⁻¹]	-1.38 1.62	-1.51 1.68	0.13 0.94	-3.15 0.79	5.12 3.68	4.05	4.20	0.84
	Melt (in mm/day) SW_{net} [W m ⁻²]	3.38 28.7	3.57 27.7	-0.19 1.9	-4.66 10.9	2.94 14.2	31.9	32.0	0.9
land	T_s (in K) [K]	267.3 258.4	267.1 257.9	-0.2 1.5	-0.9 0.1	2.2 5.1	267.5	267.3	1.2
	SW_{net} (in W/m ²) SMB [mm day ⁻¹]	62.2 1.27	65.7 1.25	-3.5 1.03	-14.3 0.67	8.2 1.56	1.09	1.00	1.09
	SMB (in mm/day) M [mm day ⁻¹]	0.15 2.18	-0.05 2.04	0.20 1.14	-0.09 0.60	1.20 1.79	2.37	2.25	1.12
	Melt (in mm/day) SW_{net} [W m ⁻²]	1.38 46.8	1.27 47.3	0.11 0.4	-1.00 20.7	0.63 22.6	61.7	65.6	-2.9

Comparison of SEMIC and MAR. Shown are multi-year (2098–2100) mean averages over the ice sheet and ice-free land, their mean difference, and the minimum and maximum differences. Compare also to Fig. ??.

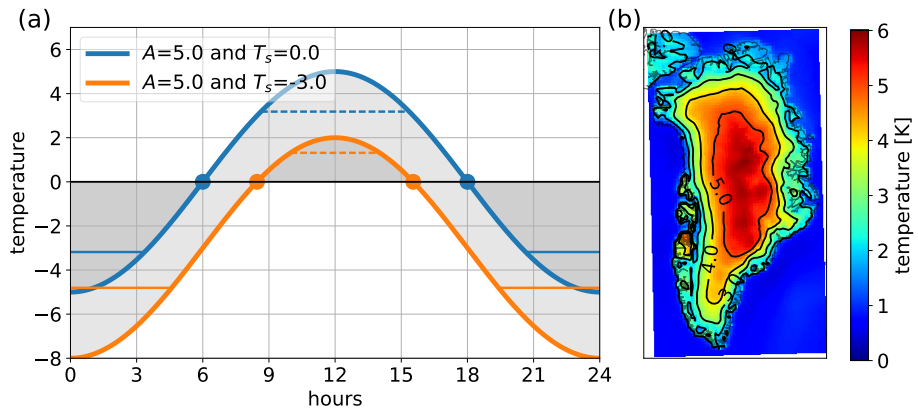


Figure 1. **Left:** The diurnal cycle parametrised as cosine function with amplitude A around the mean temperature T_s (a). The dashed horizontal line marks the analytical solution of the average above-mean temperature T_s^+ and the solid horizontal lines mark the below-mean temperature T_s^- (see Eq. 11a and b). The circles denote the roots of the sinusoidal temperature cycle curve. **Right:** The mean diurnal cycle amplitude of air temperature for the summer season (JJA) in MAR for the years 2098–21001990–1999 (b).

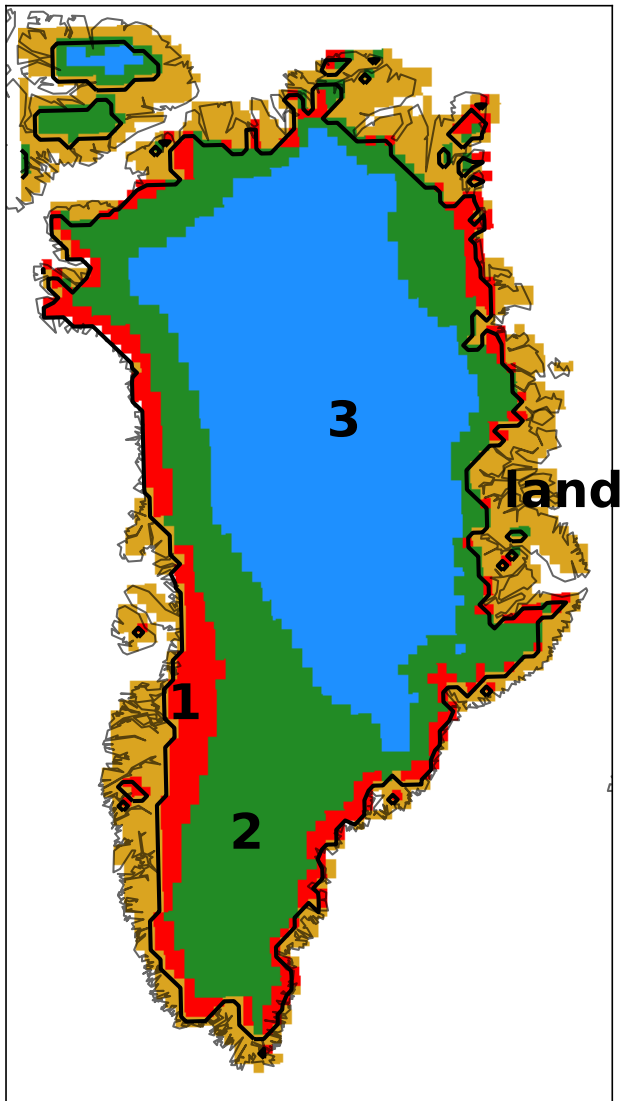


Figure 2. This region mask is used to estimate the region-averaged time series for the model calibration. Region 1 represents the ice margin, while the other regions represent areas with seasonal melt (2) or almost no melt (3). This mask is readily available from the MAR model data (named MSK). Note that these regions are only representative for present-day climatic conditions, in a strict sense. However, in a broader sense, we regard them also as useful to differentiate the future warming climatic response such under the RCP8.5 scenario.

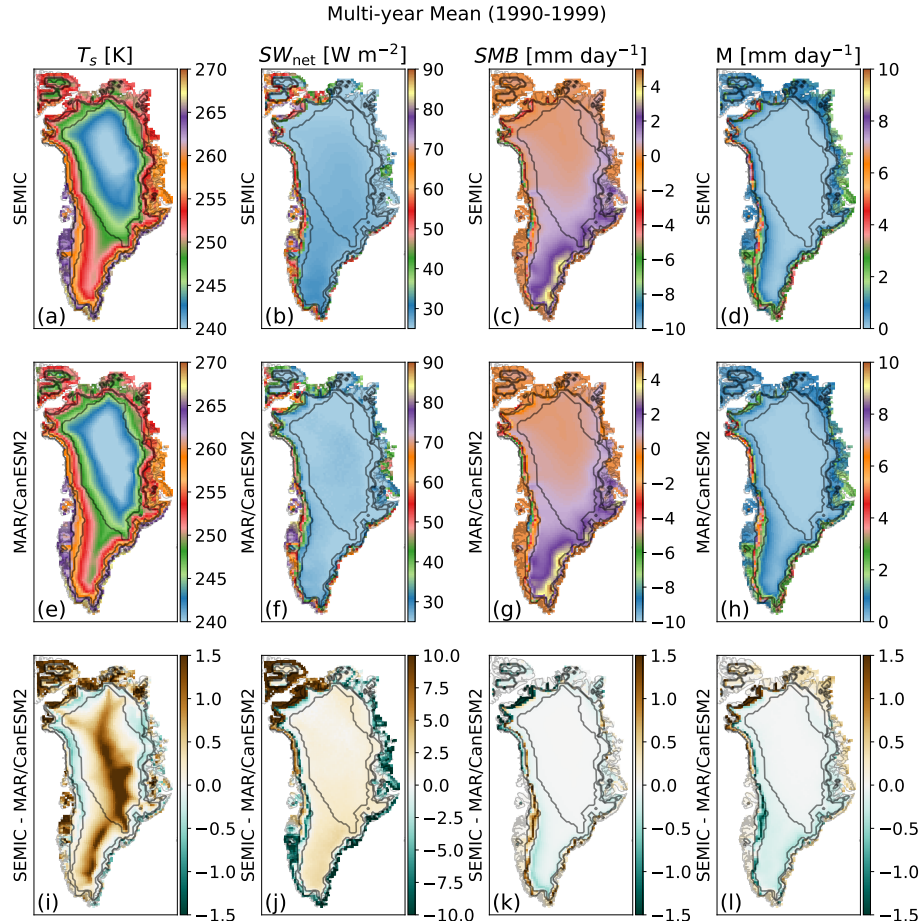


Figure 3. Comparison of modelled multi-year (1990–1999) mean surface temperature T_s , net shortwave radiation SW_{net} , surface mass balance SMB , as well as and surface melt between M as modelled by SEMIC (after model optimisation)–(d) and MAR–Differences (e)–(h) and the differences between SEMIC and MAR are depicted in the lower panels(i)–(l). The outlined contour shows contours show the boundaries of the three ice-covered MAR regions as shown in Fig. 2. See Table 4 for values of minimum and maximum differences.

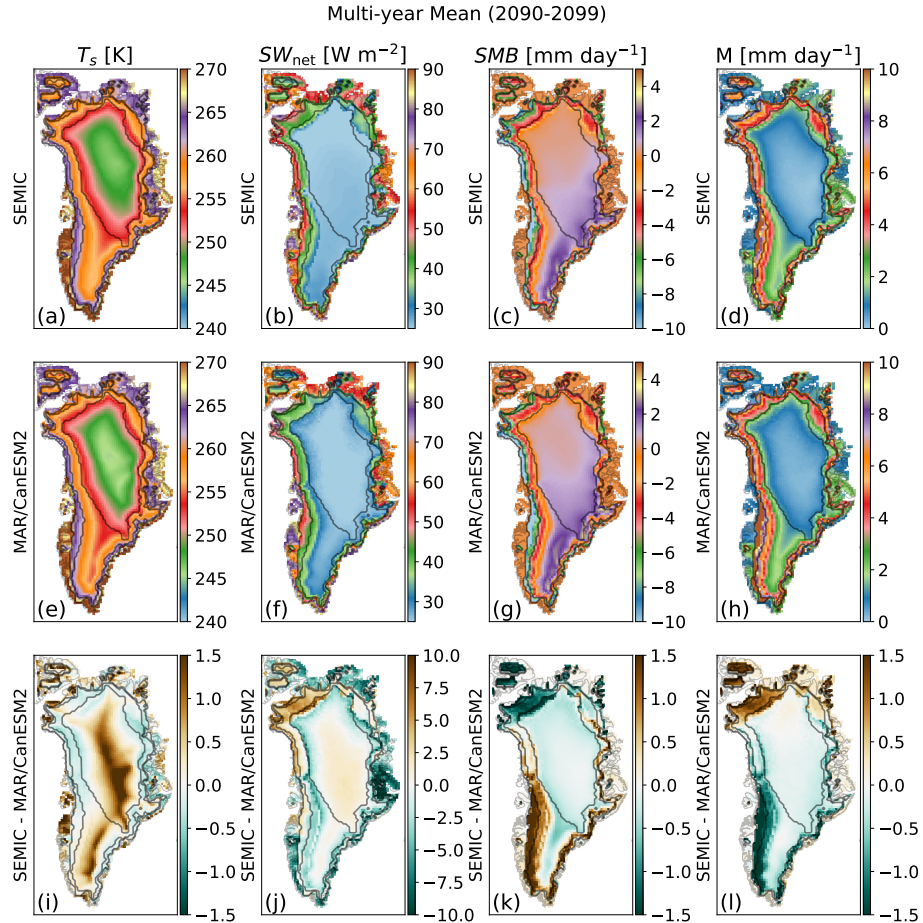


Figure 4. *Cumulative sum* Comparison of multi-year (2090–2099) mean surface temperature T_s , net shortwave radiation SW_{net} , surface mass balance over SMB , and surface melt M as modelled by SEMIC (a)–(d) and MAR (e)–(h) and the four different differences between SEMIC and MAR (i)–(l). The outlined contours show the boundaries of the three ice-covered MAR regions as defined shown in Fig. 2. See Table 4 for values of minimum and maximum differences.

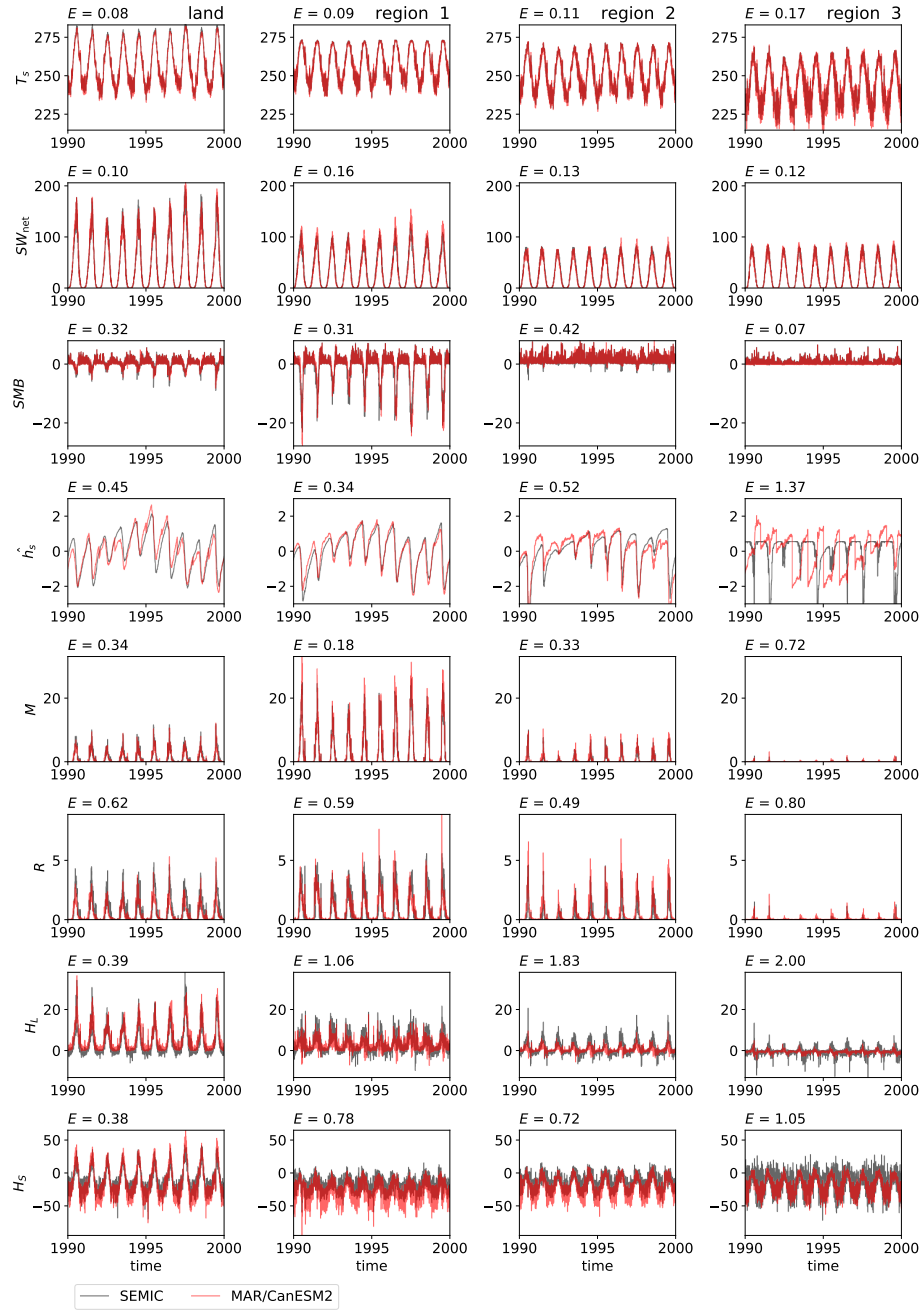


Figure 5. Time series of ice-sheet averaged surface temperature (in K) T_s [K], net shortwave radiation (in W/m^2) SW_{net} [W m^{-2}], surface mass balance (in mm/day) SMB [mm day^{-1}], standardised snow height (standardised by σ) \hat{h}_s , surface melt (in mm/day) M [mm day^{-1}], refreezing (in mm/day) R [mm day^{-1}], latent heat flux (in W/m^2) H_L [W m^{-2}], and sensible heat flux (in W/m^2) H_S [W m^{-2}] as calculated by MAR and by SEMIC with optimal parameters from Table 3 for the years 2098–2100 (=36 months) 1990–1999 of RCP8.5 the historical period. Note that h_s is scaled via its standard deviation because SEMIC and MAR incorporate a different criterion of maximum snow height (5 m in SEMIC; more than 10 m in MAR). The annotated number on the top left of each frame is the computed centered root mean square error as defined in Eq. (19) and it marks the distance to the reference field as shown in the Taylor diagram Fig. 9a.

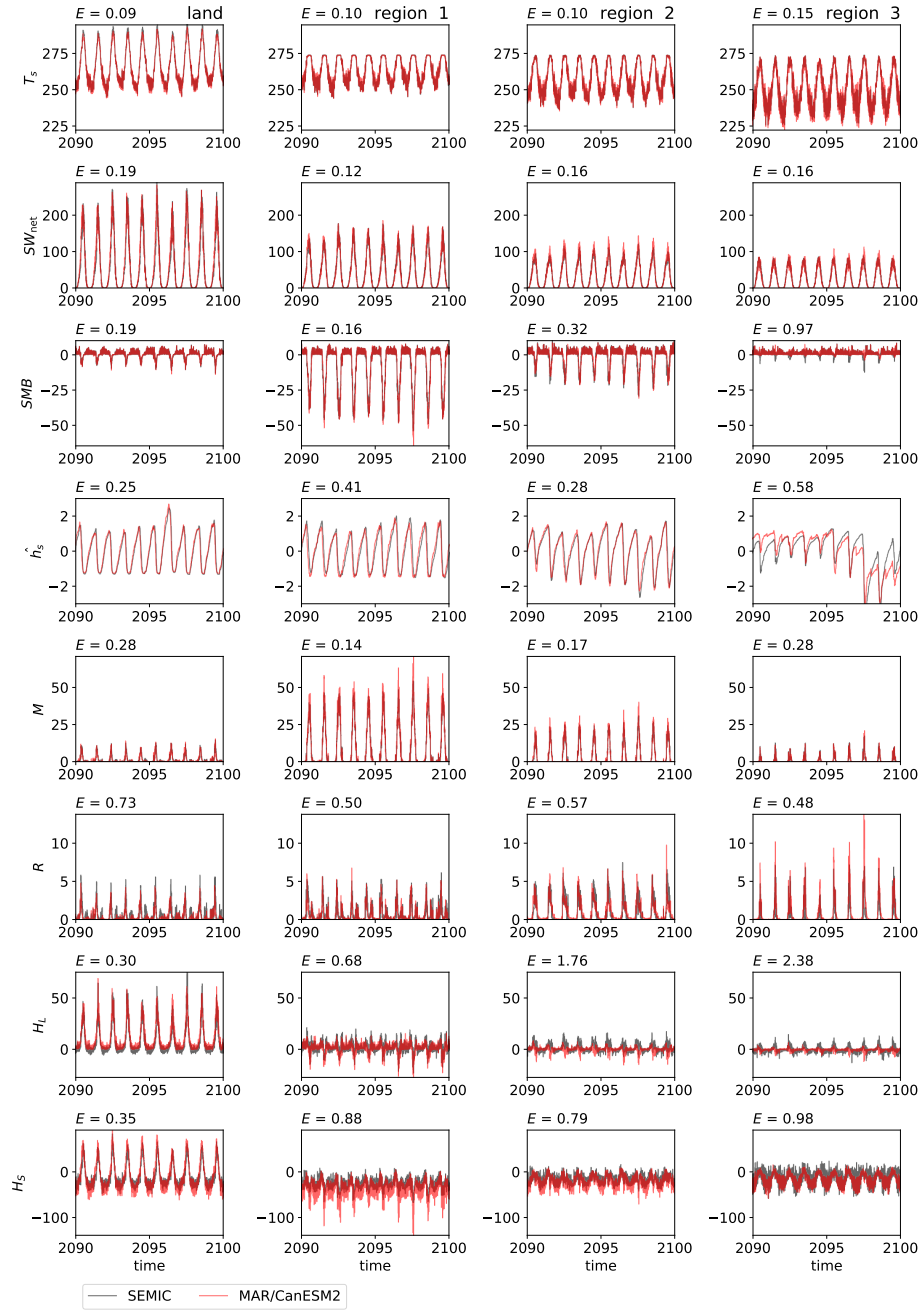


Figure 6. Time series of ice-sheet averaged surface temperature T_s [K], net shortwave radiation SW_{net} [W m^{-2}], surface mass balance SMB [mm day^{-1}], standardised snow height \hat{h}_s , surface melt M [mm day^{-1}], refreezing R [mm day^{-1}], latent heat flux H_L [W m^{-2}], and sensible heat flux H_S [W m^{-2}] as calculated by MAR and by SEMIC with optimal parameters from Table 3 for the years 2090–2099 of the historical period. Note that h_s is scaled via its standard deviation because SEMIC and MAR incorporate a different criterion of maximum snow height (5 m in SEMIC; more than 10 m in MAR). The annotated number on the top left of each frame is the computed centred root mean square error as defined in Eq. (19) and it marks the distance to the reference field as shown in the Taylor diagram Fig. 9b.

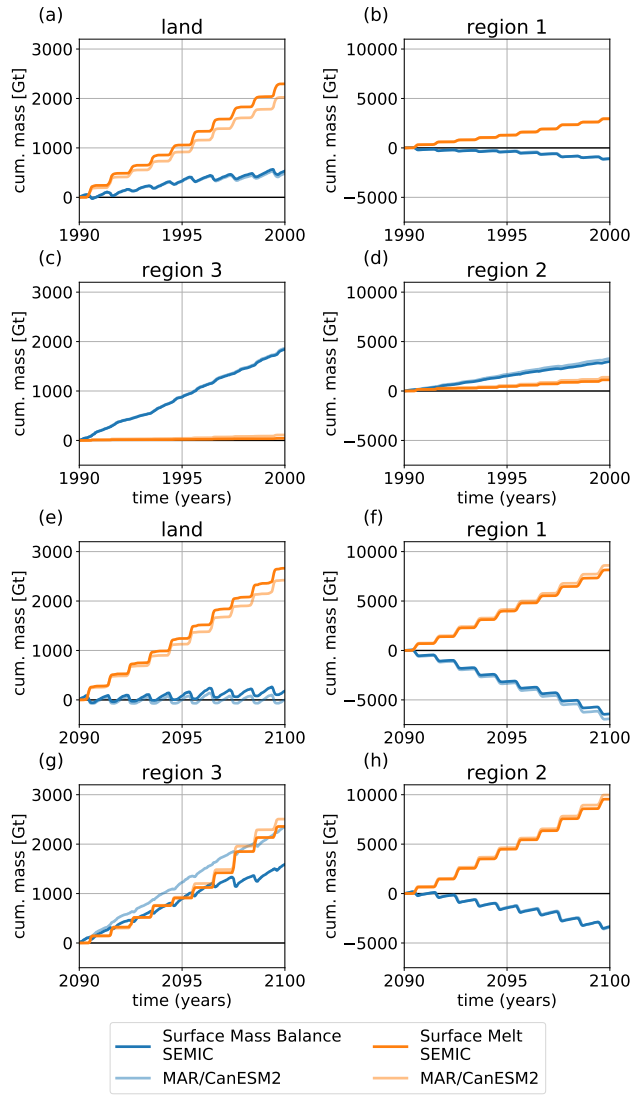


Figure 7. Cumulative sum of surface melt and surface mass balance over the four different regions as defined in Fig. 2 and both calibration periods, 1990–1999 (a)–(d) and 2090–2099 (e)–(h). Note the different y-scale for the land/region 3 (a), (c), (e), and (g) and for region 1/region 2 (b), (d), (f), (h).

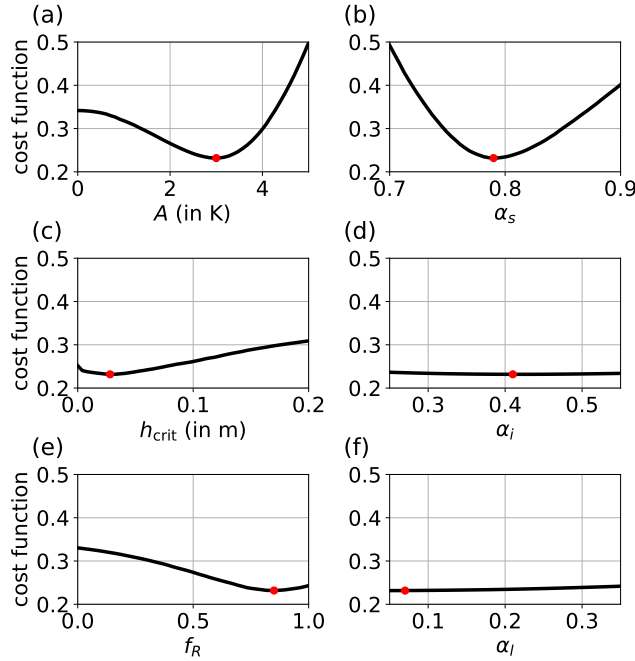


Figure 8. Sensitivity of cost function J , Eq. (20), for each of the free model parameters listed in Table 3: The diurnal cycle amplitude A (a), except α_l . Solid black lines show the total cost function snow albedo α_s (b), i.e., the root mean square of the individual cost functions. Blue indicates the cost function of the surface mass balance critical snow height h_{crit} (c), green the cost function of the net shortwave radiation bare ice albedo α_i (d), red the cost function of meltrefreezing correction parameter f_R (e), and purple indicates the cost function of the surface temperature bare land albedo α_l (f). The dashed lines red dot in each plot indicate indicates the optimum as obtained by the calibration, i.e., the particle swarm optimisation.

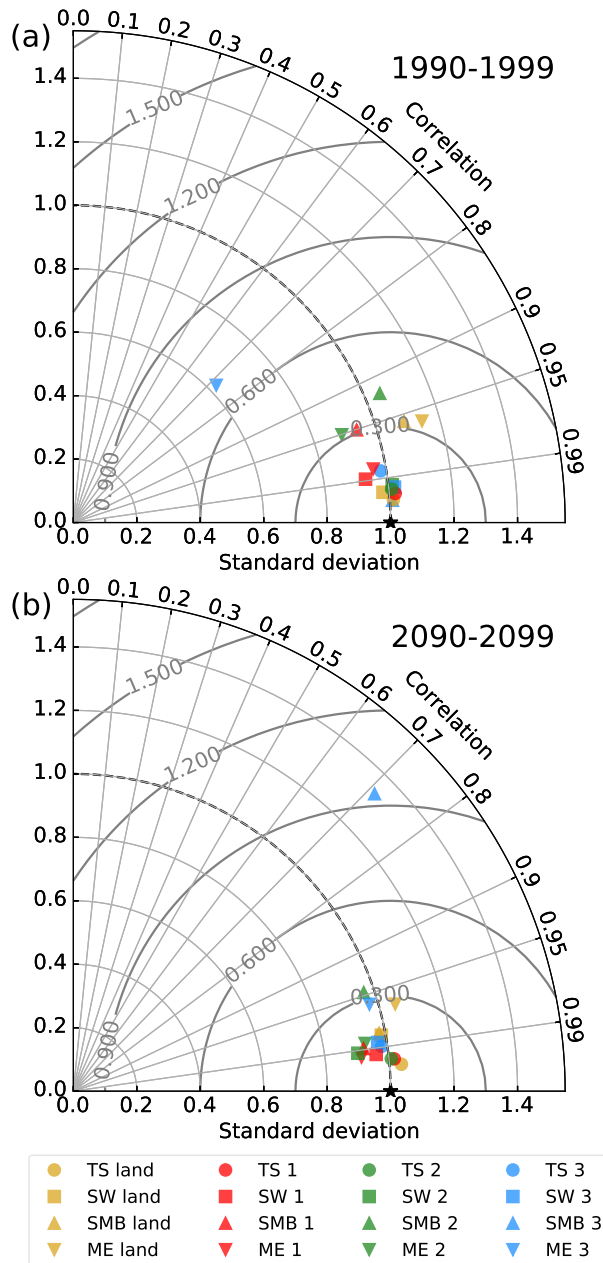


Figure 9. Taylor diagram of normalised surface temperature (TS), net shortwave radiation (SW), surface mass balance (SMB), and surface melt (ME) averaged over the whole Greenland ice sheet (as in Fig. 225 and 6) [for the historical period 1990–1999 \(a\)](#) and [for the RCP8.5 scenario, years 2090–2099 \(b\)](#). The black star denotes the reference field, which has (per definition) a standard deviation and a correlation coefficient of 1.

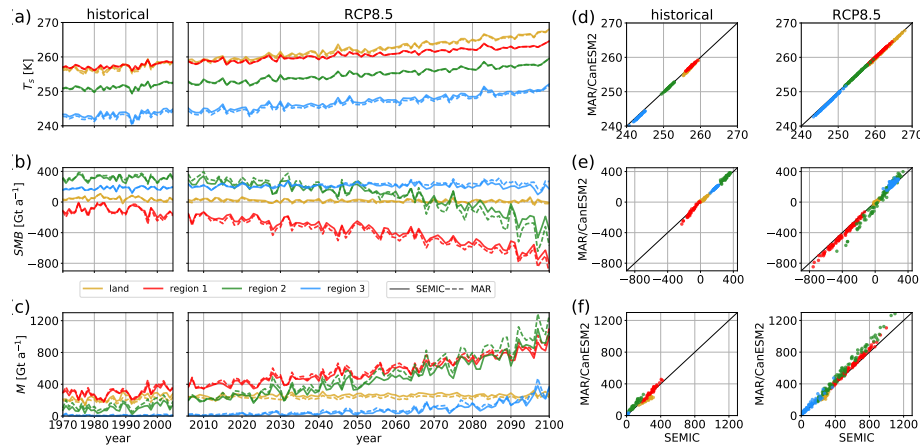


Figure 10. **Left:** Annual-mean, region-averaged surface temperature T_s (a), surface mass balance SMB (b), and surface melt M (c) for SEMIC (thick solid lines) and MAR (thin dashed lines) using the optimal parameter values from Table 3. **Right:** Point-to-point comparison of the two models (d)–(f); variables and units as in the left panel (a)–(c).

References

Bougamont, M., Bamber, J., Ridley, J., Gladstone, R., Greuell, W., Hanna, E., Payne, A., and Rutt, I.: Impact of model physics on estimating the surface mass balance of the Greenland ice sheet, *Geophysical Research Letters*, 34, L17 501, doi:10.1029/2007GL030700, 2007.

Calov, R., Ganopolski, A., Claussen, M., Petoukhov, V., and Greve, R.: Transient simulation of the last glacial inception. Part I: glacial inception as a bifurcation in the climate system, *Climate Dynamics*, 24, 545–561, doi:10.1007/s00382-005-0007-6, 2005.

Cuffey, K. and Paterson, W. S. B.: *The Physics of Glaciers*, Elsevier, 4th edn., 2010.

Dee, D. P., Uppala, S. M., Simmons, A. J., Berrisford, P., Poli, P., Kobayashi, S., Andrae, U., Balmaseda, M. A., Balsamo, G., Bauer, P., Bechtold, P., Beljaars, A. C. M., van de Berg, L., Bidlot, J., Bormann, N., Delsol, C., Dragani, R., Fuentes, M., Geer, A. J., Haimberger, L., Healy, S. B., Hersbach, H., Hólm, E. V., Isaksen, L., Källberg, P., Köhler, M., Matricardi, M., McNally, A. P., Monge-Sanz, B. M., Morcrette, J.-J., Park, B.-K., Peubey, C., de Rosnay, P., Tavolato, C., Thépaut, J.-N., and Vitart, F.: The ERA-Interim reanalysis: configuration and performance of the data assimilation system, *Quarterly Journal of the Royal Meteorological Society*, 137, 553–597, doi:10.1002/qj.828, 2011.

Fettweis, X., Franco, B., Tedesco, M., van Angelen, J. H., Lenaerts, J. T. M., van den Broeke, M. R., and Gallée, H.: Estimating the Greenland ice sheet surface mass balance contribution to future sea level rise using the regional atmospheric climate model MAR, *The Cryosphere*, 7, 469–489, doi:10.5194/tc-7-469-2013, 2013.

Fettweis, X., Box, J. E., Agosta, C., Amory, C., Kittel, C., and Gallée, H.: Reconstructions of the 1900–2015 Greenland ice sheet surface mass balance using the regional climate MAR model, *The Cryosphere Discussions*, 2016, 1–32, doi:10.5194/tc-2016-268, 2016.

Fitzgerald, P. W., Bamber, J. L., Ridley, J. K., and Rougier, J. C.: Exploration of parametric uncertainty in a surface mass balance model applied to the Greenland ice sheet, *Journal of Geophysical Research*, 117, F01 021, doi:10.1029/2011JF002067, 2012.

Franco, B., Fettweis, X., and Erpicum, M.: Future projections of the Greenland ice sheet energy balance driving the surface melt, *The Cryosphere*, 7, 1–18, doi:10.5194/tc-7-1-2013, 2013.

Gill, A. E.: *Atmosphere–Ocean Dynamics*, vol. 30 of *International Geophysics Series*, Academic Press, New York, 1982.

Greuell, W., Genthon, C., and Houghton, J.: Modelling land-ice surface mass balance, p. 117–168, Cambridge University Press, doi:10.1017/CBO9780511535659.007, 2004.

Hanna, E., Navarro, F. J., Pattyn, F., Domingues, C. M., Fettweis, X., Ivins, E. R., Nicholls, R. J., Ritz, C., Smith, B., Tulaczyk, S., Whitehouse, P. L., and Zwally, H. J.: Ice-sheet mass balance and climate change, *Nature*, 498, 51–59, doi:10.1038/nature12238, 2013.

Heinemann, M., Timmermann, A., Elison Timm, O., Saito, F., and Abe-Ouchi, A.: Deglacial ice sheet meltdown: orbital pacemaking and CO₂ effects, *Clim. Past*, 10, 1567–1579, doi:10.5194/cp-10-1567-2014, 2014.

Morin, S., Lejeune, Y., Lesaffre, B., Panel, J.-M., Poncelet, D., David, P., and Sudul, M.: An 18-yr long (1993–2011) snow and meteorological dataset from a mid-altitude mountain site (Col de Porte, France, 1325 m alt.) for driving and evaluating snowpack models, *Earth System Science Data*, 4, 13–21, doi:10.5194/essd-4-13-2012, 2012.

Moss, R. H., Edmonds, J. A., Hibbard, K. A., Manning, M. R., Rose, S. K., van Vuuren, D. P., Carter, T. R., Emori, S., Kainuma, M., Kram, T., Meehl, G. A., Mitchell, J. F. B., Nakicenovic, N., Riahi, K., Smith, S. J., Stouffer, R. J., Thomson, A. M., Weyant, J. P., and Wilbanks, T. J.: The next generation of scenarios for climate change research and assessment, *Nature*, 463, 747–756, doi:10.1038/nature08823, 2010.

Nghiem, S. V., Hall, D. K., Mote, T. L., Tedesco, M., Albert, M. R., Keegan, K., Shuman, C. A., DiGirolamo, N. E., and Neumann, G.: The extreme melt across the Greenland ice sheet in 2012, *Geophysical Research Letters*, 39, L20 502, doi:10.1029/2012GL053611, 2012.

Noël, B., van de Berg, W. J., van Meijgaard, E., Kuipers Munneke, P., van de Wal, R. S. W., and van den Broeke, M. R.: Evaluation of the updated regional climate model RACMO2.3: summer snowfall impact on the Greenland Ice Sheet, *The Cryosphere*, 9, 1831–1844, doi:10.5194/tc-9-1831-2015, 2015.

Oerlemans, J.: The mass balance of the Greenland ice sheet: sensitivity to climate change as revealed by energy-balance modelling, *The Holocene*, 1, 40–48, doi:10.1177/095968369100100106, 1991.

Oerlemans, J. and Knap, W.: A 1 year record of global radiation and albedo in the ablation zone of Morteratschgletscher, Switzerland, *Journal of Glaciology*, 44, 231–238, doi:10.3198/1998JoG44-147-231-238, 1998.

Ohmura, A.: Physical Basis for the Temperature-Based Melt-Index Method, *Journal of Applied Meteorology*, 40, 753–761, doi:10.1175/1520-0450(2001)040<0753:PBFTTB>2.0.CO;2, 2001.

Poli, R., Kennedy, J., and Blackwell, T.: Particle swarm optimization, *Swarm Intelligence*, 1, 33–57, doi:10.1007/s11721-007-0002-0, 2007.

Reeh, N.: Parameterization of melt rate and surface temperature on the Greenland ice sheet, *Polarforschung*, 59, 113–128, 1991.

Reijmer, C. H., van den Broeke, M. R., Fettweis, X., Ettema, J., and Stap, L. B.: Refreezing on the Greenland ice sheet: a comparison of parameterizations, *The Cryosphere*, 6, 743–762, doi:10.5194/tc-6-743-2012, 2012.

Robinson, A. and Goelzer, H.: The importance of insolation changes for paleo ice sheet modeling, *The Cryosphere*, 8, 1419–1428, doi:10.5194/tc-8-1419-2014, 2014.

Robinson, A., Calov, R., and Ganopolski, A.: An efficient regional energy-moisture balance model for simulation of the Greenland Ice Sheet response to climate change, *The Cryosphere*, 4, 129–144, doi:10.5194/tc-4-129-2010, 2010.

Slater, A., Pitman, A., and Desborough, C.: The validation of a snow parameterization designed for use in general circulation models, *International Journal of Climatology*, 18, 595–617, doi:10.1002/(SICI)1097-0088(199805)18:6<595::AID-JOC275>3.0.CO;2-O, 1998.

Taylor, K. E.: Summarizing multiple aspects of model performance in a single diagram, *Journal of Geophysical Research: Atmospheres*, 106, 7183–7192, doi:10.1029/2000JD900719, 2001.

Thomas, R., Frederick, E., Li, J., Krabill, W., Manizade, S., Paden, J., Sonntag, J., Swift, R., and Yungel, J.: Accelerating ice loss from the fastest Greenland and Antarctic glaciers, *Geophysical Research Letters*, 38, L10 502, doi:10.1029/2011GL047304, 2011.

van As, D., Fausto, R. S., Cappelen, J., van de Wal, R. S., Braithwaite, R. J., Machguth, H., Charalampidis, C., Box, J. E., Solgaard, A. M., Ahlstrøm, A. P., et al.: Placing Greenland ice sheet ablation measurements in a multi-decadal context, *Geological Survey of Denmark and Greenland Bulletin*, 35, 71–74, 2016.

van de Berg, W., van den Broeke, M., Ettema, J., van Meijgaard, E., and Kaspar, F.: Significant contribution of insolation to Eemian melting of the Greenland ice sheet, *Nature Geoscience*, 4, 679–683, doi:10.1038/ngeo1245, 2011.

van den Broeke, M., Bamber, J., Ettema, J., Rignot, E., Schrama, E., van de Berg, W., van Meijgaard, E., Velicogna, I., and Wouters, B.: Partitioning Recent Greenland Mass Loss, *Science*, 326, 984–986, doi:10.1126/science.1178176, 2009.

Vionnet, V., Brun, E., Morin, S., Boone, A., Faroux, S., Le Moigne, P., Martin, E., and Willemet, J.-M.: The detailed snowpack scheme Crocus and its implementation in SURFEX v7.2, *Geoscientific Model Development*, 5, 773–791, doi:10.5194/gmd-5-773-2012, 2012.